ISSN 0016-8521, Geotectonics, 2023, Vol. 57, No. 6, pp. 774–806. © Pleiades Publishing, Ltd., 2023.
Russian Text © The Author(s), 2023, published in Geotektonika, 2023, No. 6, pp. 94–129.

Khangai Intramantle Plume (Mongolia): 3D Model, Influence on Cenozoic Tectonics, and Comparative Analysis

V. G. Trifonov[a], *, S. Yu. Sokolov[a], S. A. Sokolov[a], S. V. Maznev[a], K. I. Yushin[a], and Sodnomsambuu Demberel[b]

[a] *Geological Institute, Russian Academy of Sciences (RAS), Moscow, 119017 Russia*

[b] *Institute of Astronomy and Geophysics, Mongolian Academy of Sciences, Ulaan-Baatar, PO 13343 Mongolia*

**e-mail: trifonov@ginras.ru*

Received September 14, 2023; revised October 15, 2023; accepted October 26, 2023

Abstract—The Khangai plume is situated under Central and Eastern Mongolia and is a mantle volume with significantly reduced longitudinal (*P*) wave velocities. The plume has been identified as a result of the analysis of the MITP08 volumetric model of *P*-wave velocity variations, representing the deviations of *P*-wave velocities from the average values (δVp), given as a percentage. The lithospheric mantle is thinned to ca. 50 km above the plume. Especially low velocities ($\delta Vp \le -0.6\%$) are found in the sublithospheric mantle up to a depth of 400 km. The main body of the plume is located under the Khangai Highland and extends northward to the edge of Southern Siberia. The Khentei branch of the plume that is located SE of the Khentei Highland is connected with the main plume body at depths of 800–1000 km. Branches of the plume and its Khentei branch extend into Transbaikalia. The area of the plume decreases with depth, and its deepest part (1250–1300 km) is located under the southern Khangai Highland. The main body of the Khangai plume is expressed on the land surface by the Cenozoic uplift reaching 3500–4000 m in the southern Khangai Highland. From the SE, the Khangai plume and its Khentei branch territory are limited by Late Cenozoic troughs stretching along the southeastern border of Mongolia. From other sides, the Khangai uplift is bounded by a C-shaped belt of basins. The belt includes the southwestern part of the Baikal Rift Zone, the Tunka and Tuva Basins in the north, the Ubsu-Nur Basin and the Basin of Big Lakes in the west, and the Valley of Lakes in the south. The basins are filled with lacustrine and fluvial deposits of the Late Oligocene to Pliocene. In the Quaternary, the South and Central Baikal Basins, which existed as early as the Early Paleogene, became a part of the Baikal Rift, and the other basins were involved in the general uplift of the region. The structural paragenesis of the Khangai uplift and the surrounding basins is caused by the influence of the Khangai plume. On the territory above the plume, including its Khentei and Transbaikalia branches, the Cenozoic basaltic plume volcanism occurred, inheriting the Cretaceous volcanic manifestations in some places. The structural paragenesis associated with the Khangai plume is combined with the structural paragenesis produced by lithospheric plate interaction. The latter is expressed the best of all by active faults, but developed synchronously to the plume paragenesis. The active fault kinematics shows that the eastern and central parts of the region developed in the transpression conditions and the north-eastern part developed in conditions of extension and transtension. The Khangai plume is connected at depth with the Tibetan plume, which is situated under the central and eastern Tibetan Plateau north of the Lhasa block. The Tibetan plume has the shape of a funnel rising from depths of 1400–1600 km and is accompanied by thinning of the lithosphere and uplift of the land surface. The Khangai and Tibetan plumes represent a specific category of plumes. They rise from the upper Lower Mantle and differ by this from the Upper Mantle plumes and the African and Pacific superplumes rising from the core-mantle boundary. Data are presented on the possible connection of the Khangai and Tibetan plumes with the superplume branches, but independent origin of the plumes is also admitted.

Keywords: seismotomography model of the mantle, mantle plume, Cenozoic tectonics, active fault, geodynamic influence of the mantle on the Earth's crust

DOI: 10.1134/S0016852123060079

INTRODUCTION

The region under study includes mountain systems of Southern Siberia, Western and Central Mongolia, namely, the Eastern Sayan, Khangai and Khentei Highlands, Western Transbaikalia, Gobi Altai and Mongolian Altai, as well as intermontane basins associated with them (Fig. 1).

The Cenozoic structure of the region is represented by a combination of uplifts, basins and faults breaking them. Majority of faults showing signs of Late Pleistocene–Holocene activity are structurally interconnected and can be interpreted as derivatives of a single system of deformation, which is due to the interaction of lithospheric blocks.

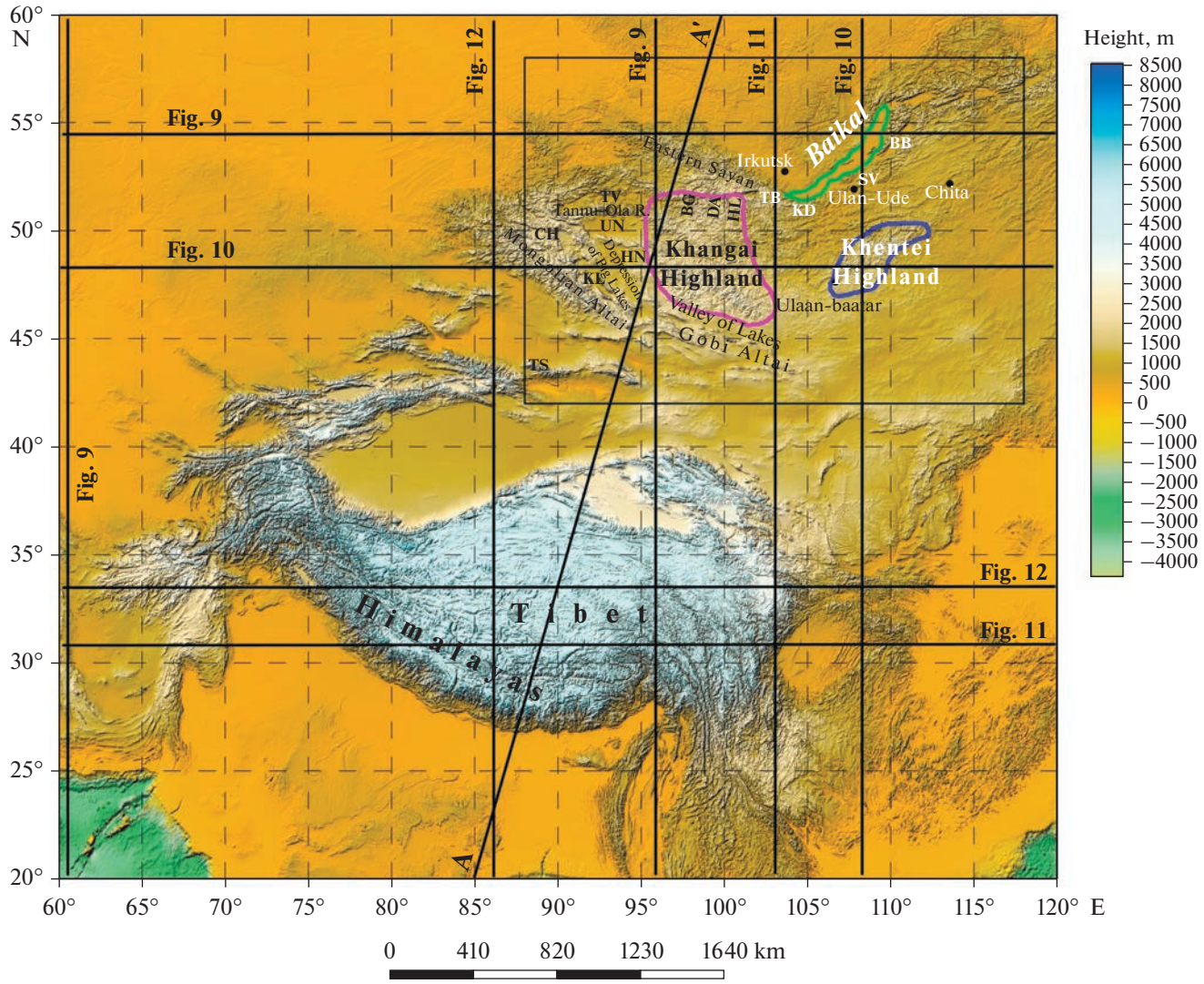

Fig. 1. Relief of Central Asia and the region of studies (rectangle, corresponding to Figs. 2, 8, 11, and 12). Position of the mantle profiles (Figs. 5–8) and contours of Baikal Lake (green), the Khangai Highland (violet), and the Khentei Highland (blue) are shown. *Basins:* (BB) Barguzin, (BG) Busiyn-Gol, (CH) Chuya, (DA) Darkhat, (HL) Khubsugul, (TB) Tunka, (TV) Tuva, (UN) Ubsu-Nur; *other symbols*: (KD) Khamar-Daban Ridge, (KL) Khara-Us-Nur Lake, (HN) Khirgiz-Nur Lake, (SV) Selenga-Vitim Trough, (TN) Tien Shan.

The origin of the Cenozoic uplifts and basins does not look so unambiguous. They are diverse in morphology, and their contours and internal structure do not always correspond to the location and kinematics of active faults. This led us to the assumption that the Cenozoic structure of the region is determined not only by the interaction of plates and blocks of the lithosphere, but also by the impact of mantle transformations. A preliminary analysis of the 3D model of *P*-wave velocity variations MITP08 [92] was undertaken. The analysis revealed a vast volume of the mantle with significantly reduced *P*-wave velocities under the Khangai Highland and its surrounding, which, narrowing, can be traced to a depth of ca. 1250 km. A channel was identified at depths of ca. 800 km, which connects the indicated volume with a similar smaller volume near the Khentei Highland. We interpreted the entire low-velocity mantle area as the Khangai intramantle plume [56].

The purpose of this paper is to determine the relationship of the Khangai plume and the Cenozoic structure of the Earth's crust in the region. To do this, the contours of the plume will be refined, its internal structure will be determined, and a 3D model will be built based on the MITP08 database; and the Cenozoic structure and its development above the Khangai plume and its surrounding will be characterized by analyzing the relief and sections of deposits in the intermontane basins. An additional goal is to determine the place of the Khangai plume in the hierarchy of plume-type mantle structures by comparing it with other plumes.

DATA USED AND METHODS OF STUDIES

To select the seismic tomographic model most suitable for analyzing the structure of the mantle of Central Asia, we constructed three meridional sections along the line A–A', based on different global models of variations in seismic wave velocities δV (Fig. 2).

With different details and configurations of boundaries, all three sections demonstrate two large mantle volumes with negative δV and signs of roots in the lower mantle are distinguished. We identified the northern volume with the Khangai plume, and the southern volume with the Tibetan plume.

The NGRAND model for *S*-waves [71, 82, 108] (see Fig. 2, section 1), calculated at the end of the 1990s, has a low resolution, but shows that the indicated features were already reliably determined at that time. It is quite applicable to illustrate the distribution of δVs on the scale of the entire Earth.

The MITP08 model for *P*-waves [92] (see Fig. 2, section 2), according to its authors, has a spatial resolution of ~100 km in the regions of the mantle with the densest data and ~150 km in the lower mantle. In it, volumes with negative δVp acquire a vertically stratified appearance and a more distinct expression of roots in the lower mantle. The UU-P07 model for *P*-waves [65, 83, 109] (see Fig. 2, section 3), according to its authors, also has a spatial detail of ~100 km near the surface and ~200 km in the lower mantle. Small-scale patterns of δVp distribution are preserved; anomalies are clearly visible in the upper mantle, but less detailed in the lower mantle. At the same time, the southern and northern parts of Tibet in the UU-P07 model have δVp variation values characteristic of the Indian subcontinent. In connection with the above, the MITP08 model [92], which has good resolution in the upper mantle and realism, was chosen for the study.

The MITP08 δVp model [92] has an improved resolution under orogenic belts, subduction zones and areas with a developed seismological network. The velocity pattern of the upper mantle of seismically active regions, which include the region of the Khangai plume and Tibet, has the spatial resolution up to 100 km in both vertical and horizontal directions [92] and the worse resolution in the lower mantle, where the density of rays from the source to the oscillation receiver is reduced. In oceanic regions, where seismicity is an order of magnitude lower than in subduction zones and continental mobile belts, as well as in the lower mantle of continents, the resolution of the MITP08 model differs insignificantly from the models of the 1990s.

The field of velocity variations can have several interpretations: thermal, mineral and strain sensitivity. The thermal model is the most valid and frequently used. Negative values of velocity variation correspond to "hot" volumes of the mantle, representing the heated and partially melted volumes. Positive values correspond to "cold" volumes, which are either the background state [51] or slabs with sufficiently large (>0.75%) positive deviations.

The data from the MITP08 model, which has an uneven depth distribution, was transformed into a 3D volumetric grid on a uniform 50 km net with redundant spacing. The grid covers the space from the land surface to the mantle-core boundary. For our work, we extracted the MITP08 data for the territory shown in Fig. 1. We analyze the spatial distribution of negative "hot" δVp. Visualization of the entire volume of the model as a 3D imagery is possible in an interactive mode, but it is difficult to show in the form of 2D illustrations. The majority of works using seismic tomography contain 2D vertical sections or horizontal slices to illustrate the properties of mantle objects. Forming of a 3D perception is difficult by this way.

One of the effective options for displaying the spatial distribution of velocity variations is a combination of two or three mutually perpendicular sections, the intersection area of which is focused on the analyzed mantle object, as shown in [52]. However, the area between the sections is not illustrated and retains uncertainty in its interpretation. In this case, a combination of sections and an isosurface of some value of the analyzed parameter can be used. This gives a possibility to trace the distribution of anomalies by the simultaneous illustration of the nominal values and their continuation into the volume between the selected section planes. This approach is used in our paper to reveal chains of "hot" mantle cavities united into continuous trajectories in the vertical and horizontal directions and contoured by an isosurface with a negative value of –0.22%. The latter was selected in such a way that the supply channels of the "hot" mantle substrate were visible from the depth to the surface. Illustrations of 2D projections of the 3D model were drawn from the most informative angle, at which the properties of the mantle that are of interest to us become visible.

The Cenozoic structure of the Earth's crust in the region was studied by analyzing numerous published materials, supplemented by new data of the authors of the paper. These new data were obtained as a result of field works of 2020–2022 and processing of field research materials, together with space images and topography models. As results of these field works, the sections of the Neogene-Quaternary deposits and interpretation of tectonic development of the Ubsu-Nur and Tuva Basins, the Depression of Big Lakes, the uplifts of the Tannu-Ola and Khan-Khuhein Ridge, and the Khangai Highland were refined, and the data were obtained on the structure and kinematics of the South Tannu-Ola, Erzin-Agardag, and Tsetserleg active faults, their relationships with the Ubsu-Nur Basin boundary and the Hangai Highland.

When assessing the structure and intensity of the Cenozoic uplifts, it was assumed that they arose at the site of a denudation or accumulative peneplain, which

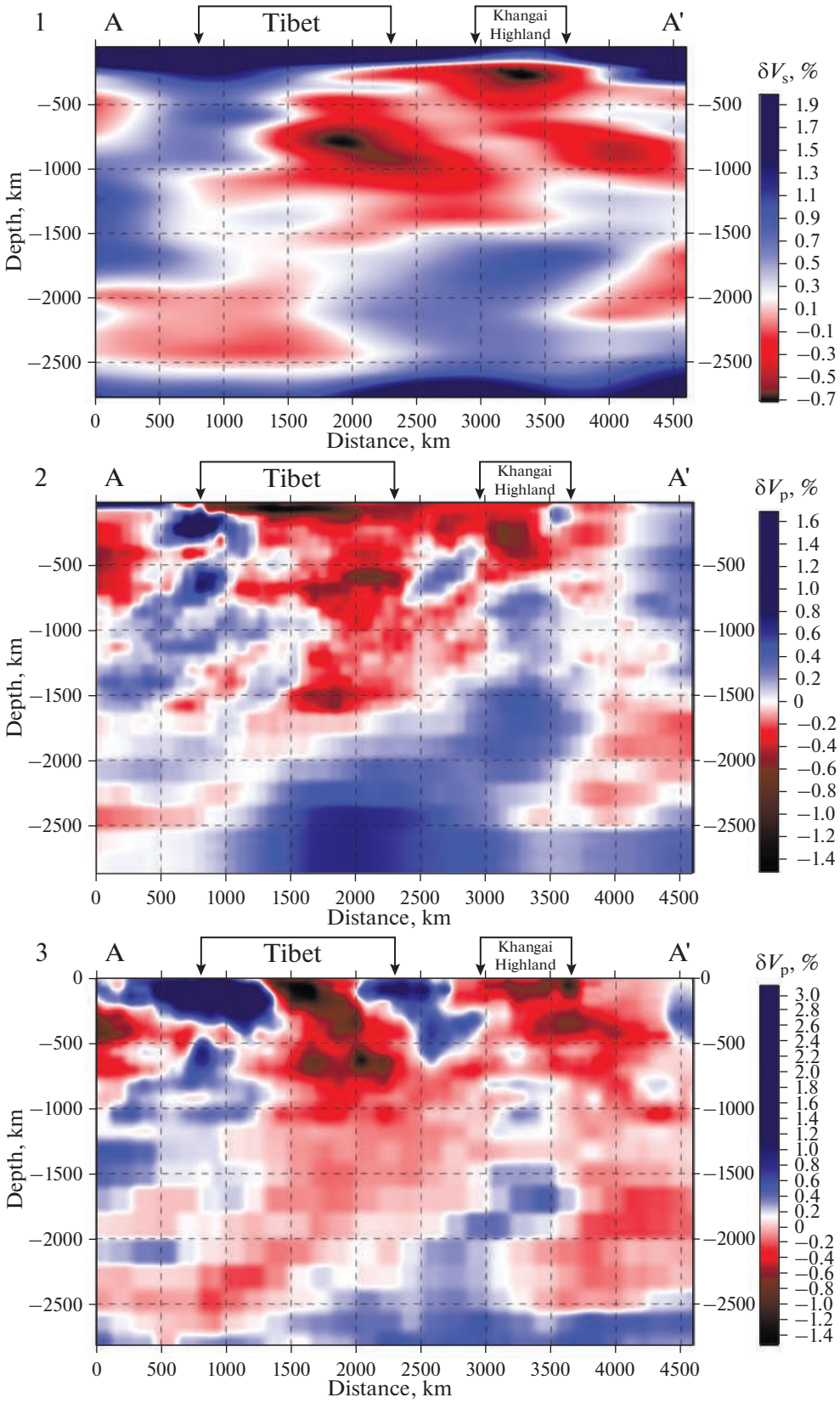

Fig. 2. Sections of the mantle along the line A–A'. The sections are based on the seismotomography models: 1 – NGRAND [71, 82, 108]; 2 – MITP08 [92]; 3 – UU-P07 [65, 83, 109].

was finally formed at the end of the Cretaceous and Paleogene. The structure of the uplifts was determined from the position of the summit plane of outcrops of the Paleozoic, less often Early Mesozoic, basement, locally covered by a weathering crust or flows of Late Cenozoic basalts. For such an assessment, geomorphological profiles were built. The structure and the history of formation of the Cenozoic basins were determined by analyzing their morphology and deposits. Changes in the particle-size distribution and provenance of the Cenozoic clastic material were indicators of the growth of uplifts. When parameterizing active faults, in addition to analyzing the published data, we identified the fault zones on space images and took into account the results of trenching.

NEOTECTONICS OF THE REGION

Pre-Cenozoic Structure

The continental crust of the region consists of the Precambrian blocks, separated and partially reworked by later tectonic formations (Fig. 3). They are relics of the Paleo-Asian Ocean, which developed from the Late Precambrian to the Early Paleozoic. The crust was consolidated approximately at the boundary of the Silurian and Devonian and was disturbed again in the south and east of the region by the formation of Hercynian and Early Mesozoic folded-thrust tectonic zones that arose during the closure of the Paleo-Tethys and Mongolian-Okhotsk paleo-oceans [30]. The Early Mesozoic zones include the Solonker zone in southern Mongolia, which experienced fold-thrust deformation in the middle Triassic [30] and the western end of the Mongolian-Okhotsk collision belt in Transbaikalia, which was formed to the middle of the Jurassic [2]. Even before the completion of these collisional processes, the NE-trending grabens arose in Western Transbaikalia, the development of which was accompanied by rift-type volcanism and ended in the middle Cretaceous [2, 62, 63, 113]. Contrasting Post-Middle Jurassic and Pre-Upper Cretaceous tectonic movements also occurred in the more western parts of the study region [7].

In the Late Cretaceous, the intensity of tectonic movements weakened and the emerging relief was largely denuded [19, 28]. The final stage of the tectonic development of the region began. It is described below.

Cenozoic Structure

The region is characterized by high relief contrast. The maximum heights are 3492 m in the east of the Eastern Sayan, 4031 m the southern Khangai Highland, 4356 m in the NW and 4231 m in the SE of the Mongolian Altai. The height of the Gobi Altai decreases from the junction with the Mongolian Altai to the east, where its maximum altitude is 2846 m. In Transbaikalia, the maximum height of 2840 m is recorded in the Barguzin Ridge. The lowest position of the land surface is at the bottom of Baikal Lake south of Olkhon Island (–1186.5 m below world sea level). Thus, the maximum contrast of the relief exceeds 5.5 km.

The Cenozoic structure of the region is formed by a combination of grabens, irregularly shaped basins, and mountain uplifts, which are bounded and dissected by faults of different kinematics. Two types of Cenozoic uplifts are distinguished: isometric arches and linear arch-block uplifts (Fig. 4).

The arched type is represented by the Khangai and Khentei Highlands. The surface of the basement, exposed on the Khangai Highland, forms a dome in the topography. The dome is divided into the northern and more elevated (up to 4000 m) southern parts by the depression between the Khangai and Tsetserleg Faults. The southern part of the dome (Khangai Ridge) is slightly elongated in the NW direction. Its southwestern slope is steeper than the northeastern one and is a plain tilting towards the Valley of Lakes. The surface is slightly deformed, and its dissection by river incisions does not exceed 500 m. The northern boundary of the southern part of the arch is expressed by a scarp, along which the surface drops by 500–750 m. The northern part of the arch, up to 3000 m high, extends to the Khubsugul Lake area and is complicated by deformation zones of the second order, forming the uplifts of the Tarvagatai, Bulnai and Khamar-Daban Ridges. The Khentei arch is similar to the Khangai arch, but smaller in size and height (up to 2800 m).

The arch-block form of linear uplifts of the second type is determined by a combination of bending of the basement surface and its block displacement and tilting as a result of movement on faults. Displacement on longitudinal faults is present in all linear uplifts. The portion of bending varies. It dominates in the Gobi Altai and is present in the Mongolian Altai and the Tannu-Ola, Khamar-Daban and Ikat Ridges. In the Eastern Sayan and the adjacent part of the Tuva Highland, the block displacement on faults dominates. Block movements determine also the horst structure of the Primorsky and Baikal Ridges on the western coast of Baikal, as well as the Barguzin and other ridges associated with grabens in Western Transbaikalia [57].

Two types of Cenozoic basins in the region are represented by grabens and basins of irregular form. The largest and most complex graben is the NE-trending Baikal Rift Zone (Fig. 5). It is bounded to the NW by a system of large normal faults separating the Baikal zone from the horsts of the Primorsky and Baikal Ridges. The opposite side of the rift is ruptured by numerous low-magnitude normal faults. The South, Central, and North Basins are distinguished within the rift zone. The depth of the lake is maximum in the northern part of the Central Basin (–1637 m relative to the water level of 455.5 m). The maximum depth is slightly less in the South Basin and much less in the North Basin.

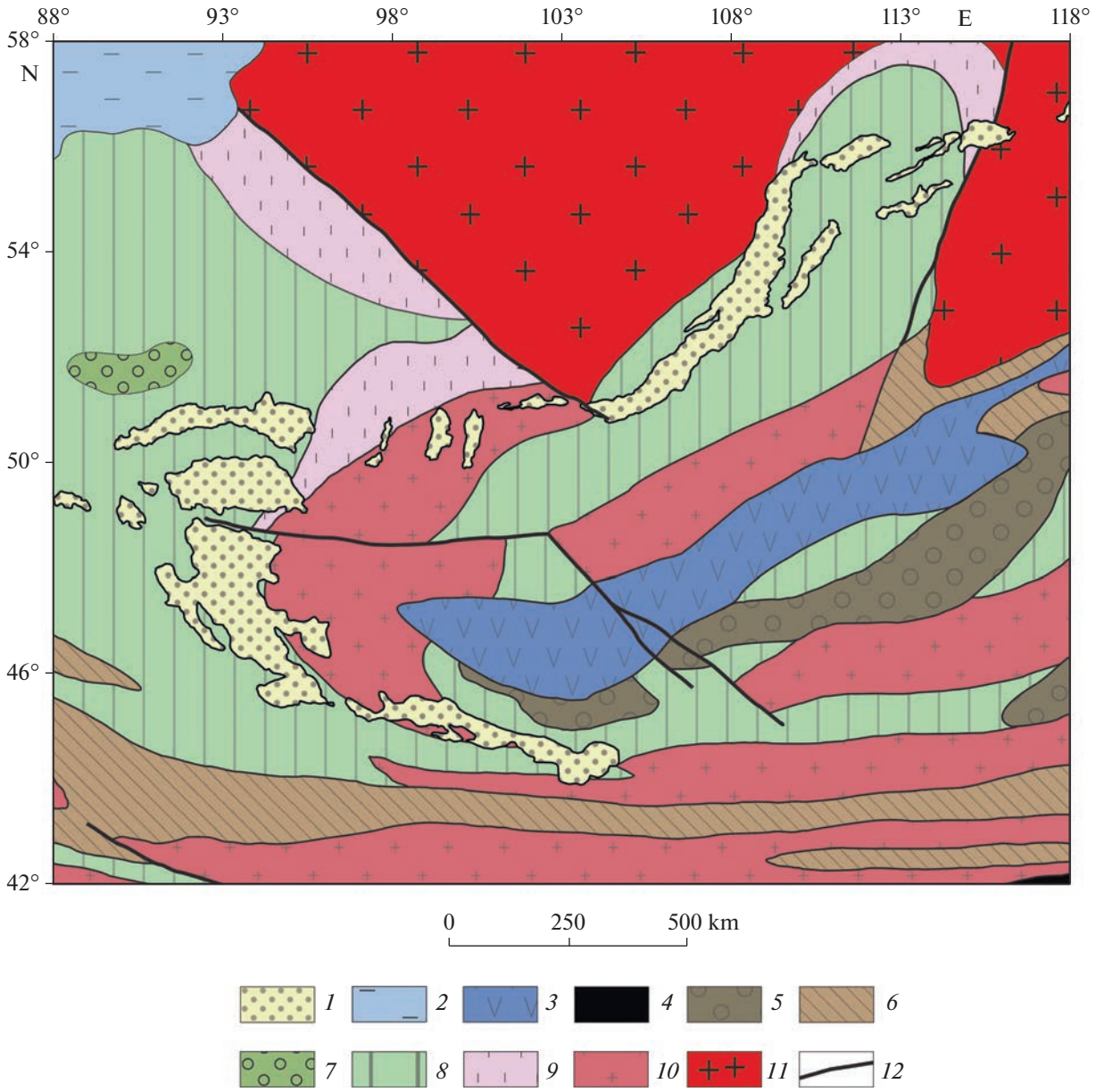

Fig. 3. Tectonic map of northern Central Asia, after [2, 30, 35] with changes and additions. *1* – Late Cretaceous and Cenozoic intermontane basins and grabens with molasses filling; *2* – Mesozoic and Cenozoic platformal cover on the deformed Paleozoic basement; *3* – Mongolia –Okhotsk Mesozoic folded-thrust belt; *4* – Solonker–Linsi Earlier Mesozoic folded-thrust zone; *5* – Hercynian residual or superimposed basins; *6* – Hercynian folded-thrust zones; *7* – Caledonian residual basins; *8* – Caledonian and Early Paleozoic folded-thrust zones; *9* – Late Proterozoic folded-thrust zones with fragments of basement of Siberian Platform; *10* – microplates and blocks of Precambrian basement in Paleozoic and Early Mesozoic folded-thrust belts; *11* – Precambrian platform; *12* – major faults.

The depocenters of the Cenozoic sedimentary cover approximately coincide with the bottom depressions. The calculated thickness of sediments reaches ca. 7 km in the South Basin and 7.5 km in the Central Basin [58]. The maximum contrast between the position of the basement surface in the north of the Central Basin and the top of the neighboring northern part of the Primorsky horst-ridge exceeds 10.3 km. The maximum height of the Baikal horst-ridge located to the NE is 2574 m, but it is only ca. 7 km higher than the basement surface at the bottom of the neighboring North Basin, where the thickness of sediments is reduced to 4.4 km [58]. The North Basin is separated from the Central Basin by the NE-trending sowneck striking from Olkhon Island to the underwater Akademichesky Ridge. The depth of the lake and the thickness of sediments are sharply reduced on the sowneck. The depth of the lake also decreases between the Cen-

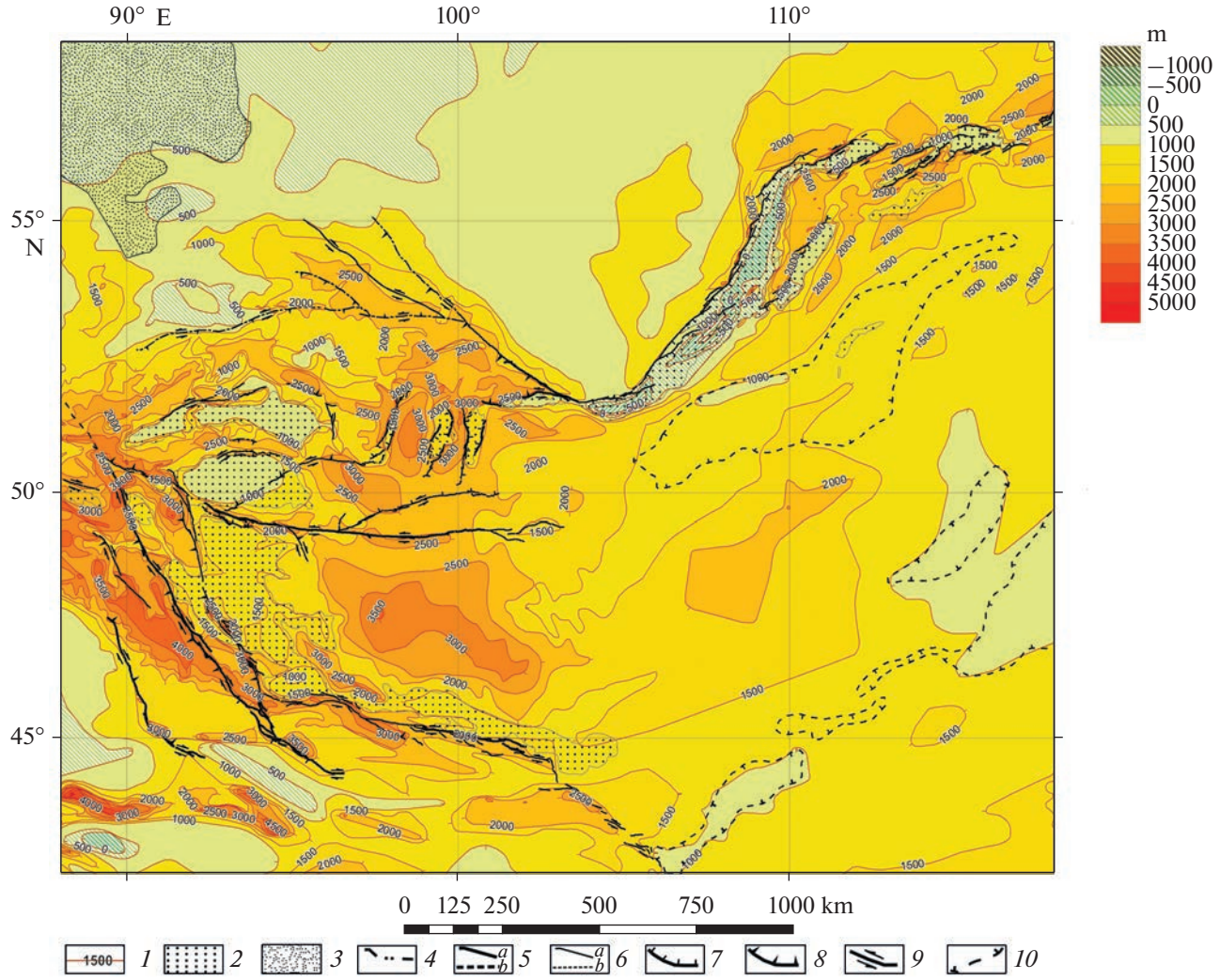

Fig. 4. The map of Cenozoic tectonics of northern Central Asia. *1* – isolines of a summit plane of the basement in uplifts and a bottom of sedimentary cover in the basins (m); *2* – sedimentary and volcanic filling of the Late Mesozoic and Cenozoic basins and grabens; *3* – plains with the Cenozoic platformal cover; *4* – Pliocene–Quaternary faults; *5* – major active faults: a – proved, b – assumed; *6* – other active faults: a – proved, b – assumed; *7* – normal faults; *8* – thrusts and reverse faults; *9* – strike-slip faults; *10* – boundaries of weakly subsided linear troughs (Selenga-Vitim and of Eastern Mongolia).

tral and South Basins, but the thickness of sediments in the Selenga River delta is increased to 7.5 km [58]. This significantly reduces the depth of sowneck.

The NE-trending grabens dominate to the east of Baikal. As a rule, they are qualified as semigrabens, in which one side is formed by a master fault zone, while the other side is not broken or is broken by faults of a smaller magnitude. More often, the master fault zone limits the graben from the NW, separating it from the adjacent horst. The large, but low-magnitude Selenga-Vitim trough has the same strike. Three N-trending grabens, Khubsugul, Darkhat and Busiyngol, are located at the northern end of the Khangai dome. The Khubsugul graben joins in the north with the Tunka-Mondy fault zone that extends eastward to the southern end of the Baikal rift zone. The bottom of the lake that fills the Khubsugul graben is at altitude of 1380 m that is more than 1 km below the surface of the ridges bounding the graben.

An important feature of the central part of the region is the C-shaped belt of basins framing the Khangai Highland from the south, west, and north (Fig. 4). All basins are expressed as depressions in the recent relief. Their bottoms are at different heights: from 980 m in the east to 1300 m in the west of the Valley of Lakes, 1200 and 950 m, respectively, in the northern and southern branches of the western Valley of Lakes NE of the junction of the Gobi Altai and Mongolian Altai, 1020 m in the Basin of Big Lakes, 750 m in the Ubsu-Nur Basin, and 700 m in the Tunka Basin. The basins differ in outline and structure.

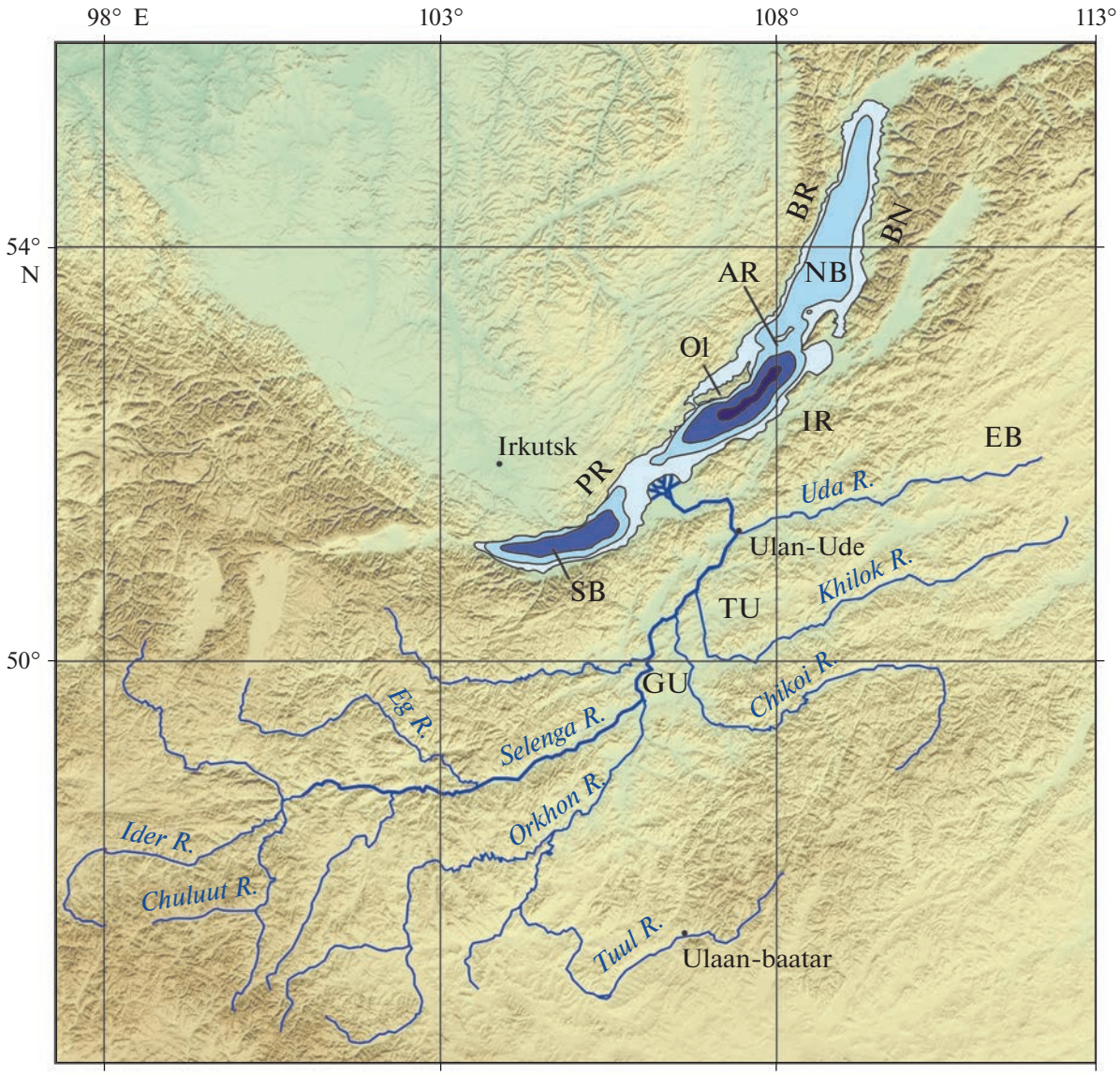

Fig. 5. The Cenozoic structure of the Baikal rift zone and its southern surrounding. *Ridges*: (AR) Akademichesky, (BN) Barguzin, (BR) Baikal Ridge, (IR) Ikat, (PR) Primorsky; *basins*: (EB) Eravna, (GU) Gusinoozerskaya, (NB) North Baikal, (SB) South Baikal (TU) Tugna Basin; (OI) Olkhon Island.

The WNW-trending southern Valley of Lakes Basin, extends between the Khangai Highland and the Gobi Altai. The thickness of the Cenozoic exceeds 600 m [6]. The northern side of the basin smoothly passes into the tilted plain of the southern slope of the highland. The Gobi-Altai fault zone extends along the southern side of the basin [55]. To the west, at the junction of the Gobi Altai and Mongolian Altai, a single valley is divided into two branches by a basement ledge.

The Basin of Big Lakes, located to the north, is an unevenly sagging depression of irregular shape. The thickness of the Cenozoic reaches 500 m according to drilling data in the north and west of the basin near Khirgis-Nur and Khara-Us-Nur Lakes. The western boundary of the basin with the Mongolian Altai is formed by a discontinuous zone of dextral strike-slip faults with a significant vertical component. The western sides of the faults are uplifted. In the north, the uplift of the Khan-Khukhein Ridge separates the Basin of Big Lakes from the Ubsu-Nur Basin. Along the southern slope of the ridge, Deviatkin [7] reported thrusting of the basement rocks over the Jurassic deposits and the Jurassic deposits over the Pliocene–Quaternary ones.

The Ubsu-Nur Basin has irregular outlines. The total thickness of the Cenozoic reaches 700–900 m in the NW and 500 m in the SW near the town of Ulangom, according to drilling data [6]. In the east, the depression borders on the spurs of the Khangai Highland without visible faults. The Khangai Fault extends

on the southern boundary of the basin, along the Khan-Khukhein Ridge. The fault is characterized by the Late Pleistocene and Holocene intense sinistral strike-slip displacement. However, judging by the presence of a near-fault up to 500–750 m high scarp, the vertical component of movements was significant at the earlier Cenozoic activity of the fault. The basin is limited to the north by the North-Ubsu-Nur Fault that inherits an ancient fault zone and is expressed in the Cenozoic structure by fold deformation of the Neogene deposits. The Lower–Middle Miocene sediments, that are present in the more southern parts of the basin, thin out near the fault. In the west, the basin is bounded by the Tsagan-Shibetu Fault, along which Deviatkin [7] suggests the 70-km post-Middle Jurassic dextral offset.

Most of the Tuva Basin is covered with the Quaternary deposits. Judging by the rare outcrops and drilling data, the Upper Oligocene and Neogene deposits lying below occupy only parts of the basin. The Sayan-Tuva Fault extends along the northern boundary of the basin. The fault inherits an ancient suture and is characterized by the left lateral slip with reverse component at the Late Cenozoic.

A chain of depressions separated by necks extends to the east of the Tuva Basin. They are (from west to east) the Mondy, Khoytogol, Tunka, Tora, and Bystrinskaya Basins. The latter is separated by the Kultuk neck from the western end of the South Baikal Basin. The thickness of Cenozoic deposits reaches ca. 2500 m in the largest Tunka Basin [43, 103]. The basins are asymmetric [19]. They are limited to the north by the mountain uplift of the Tunkinskiye Goltsy with heights up to 3200–3300 m. The slope of the uplift facing the basins is steep. The Tunka-Mondy fault zone strikes along it and joins in the east the southeastern end of the Main Sayan fault zone. The slope of the Khamar-Daban Ridge, which limits the chain of basins from the south, is more gentle and its plateau-like surface is 500–700 m lower than the Tunkinskiye Goltsy. The asymmetry is confirmed in the Tunka Basin by the fact that the area of the greatest thickness of deposits is close to the northern side of the basin.

The South Basin of Baikal can be considered in its location and orientation as a continuation of the C-shaped belt, but morphologically it is a part of the Baikal rift zone, which has the shape of an asymmetric graben.

En-echelon row of flat linear depressions stretches along the southeastern boundary of Mongolia from the eastern end of the Gobi Altai up to the Buir-Nur and Dalainor Lakes and the riverhead of the Argun River. The depressions are composed of the Paleogene and Miocene deposits, locally covered with the Quaternary sediments. Probably, the depressions are the southeastern element of the belt of basins that bounds the Khangai and Khentei arches.

History of Development of the Cenozoic Structure

The Cenozoic of northern Central Asia is composed of continental terrigenous deposits of different particle-size distribution and origin, in places with the participation of basalts and coal-bearing rocks at several stratigraphic levels. The Cenozoic stratigraphy of the region has been intensively studied over the past 70 years. The decisive contribution to these studies was made by the works of Logachev for the Baikal part of the region [18, 19] and Deviatkin for Mongolia [6]. The results obtained are based on the study of sections of basins and their comparison with relics of weathering crusts on neighboring uplifts.

Mats [27, 28] divided the deposits of the Baikal rift into three tectonic-stratigraphic groups:

(1) Upper Cretaceous no higher than Maastrichtian – Lower Oligocene (ca. 70–27 Ma);

(2) Upper Oligocene–Lower Pliocene (27–3.5 Ma);

(3) Upper Pliocene–Quaternary (the last 3.5 Ma).

Matz divided groups (2) and (3) into upper and lower subgroups and found the phases of deformation that occurred between the epochs of their accumulation. The phase ages are ca. 27 Ma between groups (1) and (2), ca. 10 Ma between the lower and upper parts of group (2), 4–3 Ma between groups (2) and (3), and 1.2–0.8 Ma between the lower and upper parts of the group (3). The phases are expressed by angular unconformities, structural rearrangements, and/or changes in sedimentation. We extended these groups to the entire studied region.

In the Gobi Altai area and the Valley of Lakes, the Upper Cretaceous – Lower Oligocene form the platformal cover of fine-grained sandy-clayish deposits usually red in color. They overlap with unconformity the rocks of the basement and in places Mesozoic up to the Lower Cretaceous inclusive.

The Cenozoic part of the group (1) is ca. 280 m thick in the Valley of Lakes (Fig. 6, section 1). In the axial part of the basin, a significant part of the deposits are of lacustrine origin. In the northern slope of the basin, the thickness decreases and the portion of alluvial deposits increases. The Upper Oligocene is connected by a gradual transition with the Lower Oligocene. The Oligocene of the northern slope of the basin contains three basalt beds with K-Ar dates of 32 ± 2, 31 ± 0.2 Ma, and 24 ± 3 Ma [6]. The number of basalt layers increases in the southern slope of the Khangai Highland. The Miocene is identified as the Oshin Formation in the depressions located NE of the junction of the Gobi Altai and the Mongolian Altai. It is composed of 100–150 m thick lacustrine clays and silts with limestone, sand, and gravel interlayers in the central parts of the depressions, and up to 150 m thick alluvial and lacustrine sands with clay interbeds near neighboring uplifts. To the east, in the northern slope of the Valley of Lakes, the Lower–Middle Miocene contains two basaltic layers with K-Ar dates of 20 ±

0.5 and 18.9 ± 0.8 Ma [6]. The wells uncovered the 80–100 m thick Lower-Middle Miocene lacustrine deposits in the basin center.

The Pliocene and Quaternary of the axial part of the Valley of Lakes are composed of lacustrine sediments. Their distribution area decreased over time. According to the borehole data, the thickness of the Lower Pliocene is 100–120 m and decreases towards the sides to 80 m. Starting from the Upper Pliocene, a general coarsening of detrital material and an expansion of the areas of alluvial deposits in the marginal parts of the basin are recorded. The total thickness of the Upper Pliocene and Quaternary is estimated at tens of meters. There are lake terraces of the Middle and Late Pleistocene on the shores of recent Bon-Tsagan-Nur and Ulan-Nur Lakes. The former rise at 100–200 m and the latter rise at 40–60 m above the recent levels of the lakes. Similar terraces of dry lakes are uplifted at 100–150 and 50 m, respectively, NE of the junction of the Gobi Altai and Mongolian Altai [6].

To the south of the Gobi Altai and SW of the Mongolian Altai, the Paleogene and Neogene are lithologically similar to those in the Valley of Lake. The thicknesses of the Upper Oligocene and the Neogene decrease to 20–30 and 25–30 m to the south of the Gobi Altai. The reduction in thickness indicates a weakening of subsidence. The similarity of the sections and the penetration of sediments on the slopes of the Gobi Altai testify in favor of the fact that its main part began to rise no earlier than the Miocene.

In the depressions united by the name of the Basin of Big Lakes (Fig. 6, section 2), the section begins with the 50–60 m thick Upper Oligocene red clays and sandstones. The Miocene is represented by the 200–300 m thick terrigenous Oshin Formation. Its lower part (Lower?–Middle Miocene) is similar to that in the Valley of Lakes. The upper part of the formation is composed of the 80–100 m thick sands with interlayers of marly clays in the northern shore of the Khirgis-Nur Lake. The lacustrine and alluvial deposits are replaced in the sides of the basin by subaerial clays with interbeds of sand, rubble, and pebbles [6]. Two types of sections are distinguished in the Lower Pliocene, with the uppermost Miocene and possibly the lowermost Upper Pliocene. The up to 150–200 m thick Khirgis-Nur Formation fills in the central parts of the basin. It is composed of lacustrine and lacustrine-alluvial sediments. The up to 100–150 m thick more coarse fluvial Altan-Teli Formation is characteristic for the borders of the basin.

The up to 20 m thick Upper Pliocene–Lower Pleistocene alluvial deposits (the Tuin-Gol Formation) overlie. Their analogs form covers of the 60–90 m high terraces in the slopes of the Mongolian Altai. The lower terraces belong to the Middle–Late Pleistocene. The Middle and Late Pleistocene lake terraces are elevated above the present water level at 232 and 152 m, respectively, around the Khirgis-Nur Lake [6].

In the northern Ubsu-Nur Basin, the section begins with the 120 m thick clays of the Upper Oligocene (?) [61]. The Lower and Middle Miocene are not identified in the studied sections, but are present to the south. Analogues of the upper part of the Oshin Formation (Upper Miocene), Khirgis-Nur Formation (Upper Miocene–Pliocene), and Tuin-Gol Formation (Upper Pliocene–Lower Pleistocene) are presented. The Pleistocene lacustrine deposits are presented in the center of the basin. The lake terraces of the Middle and Upper Pleistocene rise above the level of the Ubsu-Nur Lake, respectively, at 303 m and 207 m [6].

In the northern Tunka Basin, the thickness of the Cenozoic reaches ca. 2500 m south of the town of Arshan [43, 103]. The R-2 well drilled here the 2120 m thick section and did not reach the basement [89]. The surface of the basement was uncovered at a depth of 1059 m by well S-1, drilled in the southern part of the basin, where the thickness of the deposits is reduced [26]. The section of the Tunka Basin (Fig. 6, section 3) contains five stratigraphic units [43, 103]:

(1) the Upper Oligocene–Lower Pliocene Tankhoi (Coal-bearing) Formation, ca. 1400 m thick;

(2) the Upper Pliocene Ocher (Red-colored) Formation, ca. 500 m thick;

(3) the Upper Pliocene–Gelasian tuffaceous-sandy unit, 270 m thick;

(4) the Lower–Middle Pleistocene (possibly with lower Upper Pleistocene) sandy unit, 300–350 m thick;

(5) the Upper Pleistocene–Holocene, up to 30 m thick.

The Tankhoi Formation (1) is composed of clays, silts, sands, and marls. There are diatomites and brown coals near the sides of the basin and dozens of basalt lava flows in the section of borehole R-2. Basalts of the Tankhoi Formation from the borehole R-2 (the lower 1060 m of the borehole section) are dated to ages of 16 to 8 Ma [43].

The Ocher Formation (2) consists of sands, silts, clays, and rarer gravel-pebble material, the content of which increases towards the sides of the basin.

The unit (3) is composed of sands, clays, and tuff-detrital sediments with basalt layers dated in the R-2 borehole at ca. 4–2.4 Ma [43]. The content of boulder-pebble deposits increases towards the sides of the basin.

The unit (4) is composed of sands with lenses of pebbles and peat and beds of basalt and tephra. The unit contains moraines and fluvioglacial and fluvial pebbles and sands. The basalt flow near the top is dated at ca. 1.6 Ma in the section of borehole R-2, which covers only the 230 m thick lower part of the unit (4).

The sequence (5) contains fluvial and lacustrine sands and silts with peat and travertine and usually incised into the older deposits.

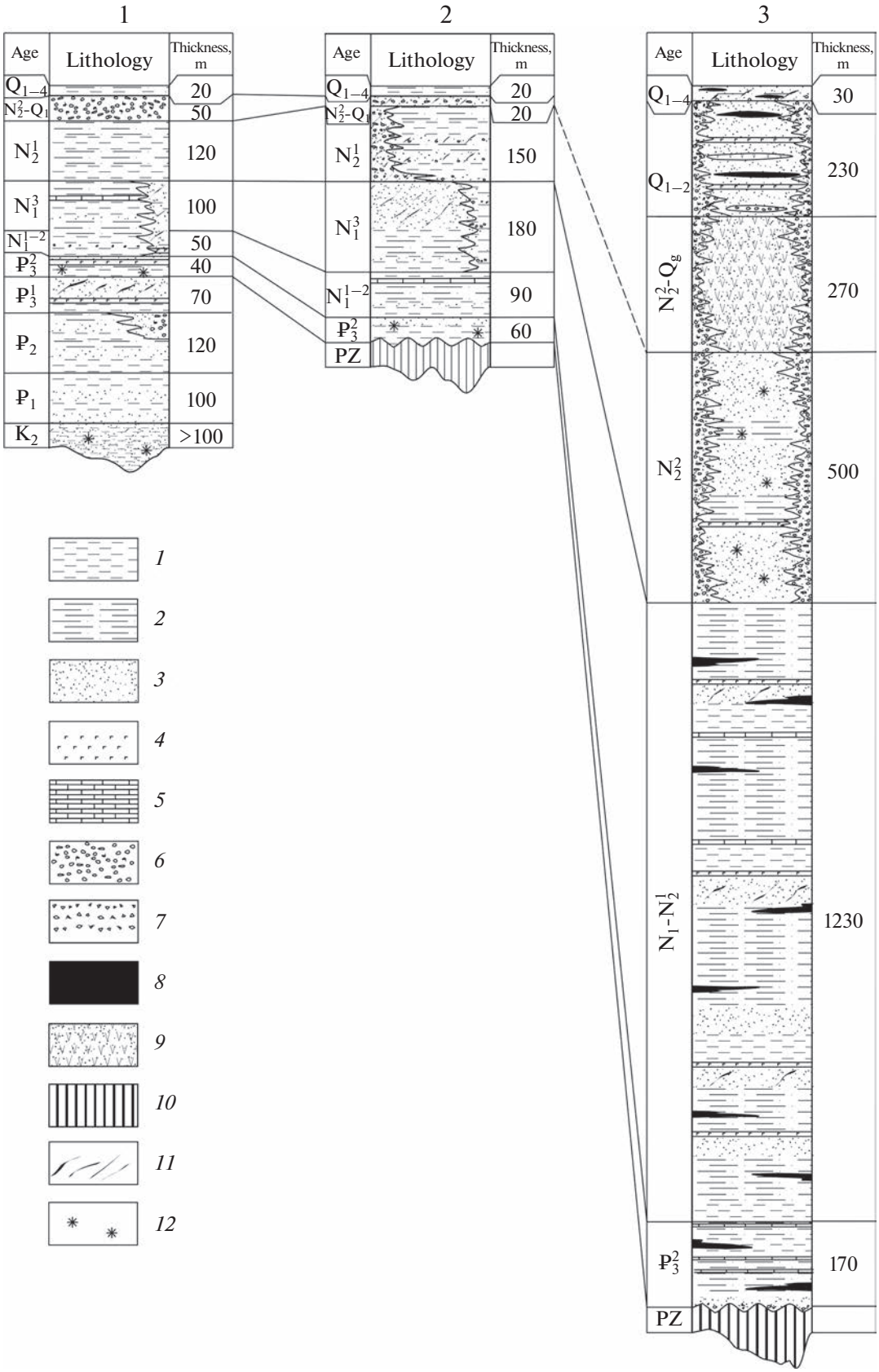
1
2
3
Age
Lithology
Thickness, m
Q_{1-4}
N_2^2-Q_1
N_2^1
N_1^3
N_1^{1-2}
P_3^2
P_3^1
P_2
P_1
K_2
20
50
120
100
50
40
70
120
100
>100
PZ
150
180
90
60
Q_{1-2}
N_2^2-Q_g
N_2^2
N_1-N_2^1
30
230
270
500
1230
170
1
2
3
4
5
6
7
8
9
10
11
12

At an early stage of studying the history of the Baikal rift zone, the presence of the Upper Oligocene–Lower Pliocene and the Upper Pliocene–Quaternary tectonic-stratigraphic groups was proved, and considerations were made about the possible presence of the Upper Cretaceous–Lower Oligocene Group at the sedimentary cover [19, 31]. A direct evidence of its presence was the discovery of the Eocene spore-pollen under the palynologically identified Neogene and Quaternary deposits in the borehole section in the Selenga River delta [9]. Since the borehole uncovered only 3100 m of the sedimentary cover, and the basement surface is located, according to seismic data, at a depth of more than 5 km, the presence of sediments up to the Upper Cretaceous seemed possible.

Seismic profiling of the Baikal basins using the method of reflected waves made it possible to identify three seismostratigraphic complexes [58]. The lower complex is seismically transparent. The middle one is layered by extended reflectors, ruptured by numerous faults. The upper one consists of extended undisturbed reflecting horizons. The boundary of the lower and middle complexes is gradual and occupies a part of the section with a thickness of tens of meters.

The depocenters coincide with the greatest depths of the lake bottom in all three basins. The lower complex is present only in the South and Central Basins, where it has the shape of a wedge, the thickness of which decreases from 4–5 km in the depocenters to several hundred meters near the southern and southeastern shores of the lake. The middle complex is 1–2 km thick. The upper complex, which is 0.3–0.5 km thick in the South and Central Basin, thickens up to 2 km in the North Basin.

Correlation of the seismostratigraphic complexes and tectonostratigraphic groups is a subject of discussion. According to the most balanced Mats' model [27, 28], the lower seismostratigraphic complex correlates to the lower tectonostratigraphic group (Upper Cretaceous–Lower Oligocene) and the lower subgroup of the middle group (Upper Oligocene–Middle Miocene). The middle seismostratigraphic complex corresponds to the upper Tankhoi Formation (Upper Miocene–Lower Pliocene), while the upper complex corresponds to the Upper Pliocene–Quaternary.

The Selenga-Vitim trough, extending from the middle reaches of the Selenga River to the Vitim Plateau, was a denudation-accumulative plain bounded from the south by an area of low-mountain relief from the Late Cretaceous to the Early Oligocene [19, 28, 41]. The southwestern part of the trough is covered with Quaternary alluvium of the Selenga and its tributaries, under which the presence of older deposits is possible.

Southward of the western part of the trough, the 5–10 m thick alluvium composes high (from 80 to 250 m) terraces of the Selenga, Chulutu, and Orkhon Rivers, incised to the northeastern slope of the Khangai Highland. The terrace alluvium is interbedded and overlain by basalts. The K-Ar dates of basalts on the 90–100 m high terrace of the Chulutu River are from 6.2 ± 0.5 to 3.1 ± 0.2 Ma [6]. The succession of terraces reflects the rise of the Khangai Highland.

In Western Transbaikalia, the NE-trending graben-like basins were formed in the Late Cretaceous and Cenozoic. The Lower Makhei and Eravnoye basins are among the early formations of this type. The central parts of these depressions are composed of fine-grained alluvial and lacustrine sediments, which are replaced towards the sides by coarser clastic deposits that were accumulated due to the erosion of the basin slopes [60]. The fine-grained plain sedimentation with records of coal formation continued in the Late Oligocene–Early Pliocene, when activation of vertical movements and basaltic volcanism took place and the Barguzin and other new graben-like basins were formed in the more northern part of Transbaikalia. Formation of new grabens continued in the Late Pliocene–Quaternary, when the recent structural pattern of Transbaikalia was finally formed.

Stages of Tectonic Development in the Region of Studies

The history of the tectonic development of the region during the Late Cretaceous and Cenozoic is reconstructed on the basis of the represented data.

The early stage. The first stage of the Late Cretaceous and Paleogene up to the early Oligocene, was the time of planation and relatively weak tectonic movements. The accumulative peneplain with thin cover of platform-type deposits was formed in the south of Mongolia up to the latitude of the southern foothills of the Khangai Highland. Probably, these deposits covered a part of the Gobi Altai, while relics of the Jurassic denudation peneplain remained in other parts of it (the Ih-Bogd Rise) and the Mongolian Altai (Baatar Range) [87]. The area of sedimentation extended to the west along the northern foothills of the

Fig. 6. Sections of the Cenozoic deposits in basins of the C-like belt around the Khangai arch: 1 – Valley of Lakes, 2 – Depression of Big Lakes, 3 – Tunka Basin. Age symbols: Q_{3-4} – Upper Pleistocene and Holocene, Q_{1-2} – Lower and Middle Pleistocene, Q_1 – Lower Pleistocene, Q_g – Gelasian, Q_{1-4} – Quaternary, N_2^2 – Upper Pliocene, N_2^1 – Lower Pliocene, N_1^3 – Upper Miocene, N_1^{1-2} – Lower and Middle Miocene, N_1 – Miocene, P_3^2 – Upper Oligocene, P_3^1 – Lower Oligocene, P_2 – Eocene, P_1 – Paleocene, K_2 – Upper Cretaceous, PZ – Paleozoic. *1* – clays; *2* – aleurites; *3* – sands and sandstones; *4* – basalts; *5* – limestone; *6* – gravel and pebbles; *7* – rubble; *8* – brown coal and peat; *9* – tuffstone; *10* – Paleozoic basement; *11* – cross bedding; *12* – red rocks.

Tien Shan, where the continental sediments were partially replaced by shallow water marine sediments.

The denudation peneplain with weathering crusts and remnants of the earlier relief developed in the more northern part of Mongolia, Tuva, and the Sayans. Fission-track analysis performed on the Chulyshman Plateau in Altai revealed a planation in the Upper Cretaceous after the Upper Jurassic–Lower Cretaceous tectonic activity [78]. The Khangai and Khentei Highlands were steadily rising, serving as sources of clastic material since the Jurassic [2]. The accumulative peneplain with weathering crusts and weak fluvial sedimentation developed in flat depressions and river valleys of the Selenga-Vitim trough, while a denudation peneplain formed on the neighboring uplands [28]. The South and Central Baikal basins subsided and the thickness of sediments reached 4–5 km in their depocenters.

The second stage. At the second stage of development, which lasted from the Late Oligocene to the Early Pliocene, the contrast of vertical movements increases due to both the formation and deepening of basins and the growth of uplifts. The C-shaped belt of basins was formed around the Khangai Highland, which continued to rise. The sediments of the second stage overlap the platform-type deposits of the first stage in the Valley of Lakes. In the more northern basins, the sediments of the second stage overlie the basement.

The thickness of deposits increases from 300 m in the Valley of Lakes, 500 m in the Basin of Big Lakes, and 700–800 m in the Ubsu-Nur depression to ca. 1400 m in the Tunka Basin. In the Baikal rift zone, the South and Central Basins of the Baikal rift continued to sink, and the thickness of the sediments reached 2 km. The future Northern Basin of Baikal began to subside and 150 m of deposits were accumulated [27]. New NE-trending graben-like basins appeared in Transbaikalia. The sediment thickness of the second stage exceeded 700 m in the largest Barguzin Basin according to drilling data [89].

Along with the subsidence of the basins, the rise of neighboring uplifts occurred. The rise of the Khangai and Khentei arches is recorded by the ongoing transportation of eroded clastic material from them. At the boundary of the Basin of Big Lakes with the Mongolian Altai, the replacement of fine-grained detrital lacustrine and alluvial deposits typical of the central parts of the basin, by coarser detrital material was revealed [6]. By the same way, the fine-grained lacustrine-marsh Tankhoi Formation of the southern coast of the Baikal Lake is replaced by the sandy-pebbly facies in the border with the Khamar-Daban Ridge [28, 42].

The third stage. During the third stage of development, lasting from the Late Pliocene to the present, the structure of the land surface gradually has acquired recent features. The continuing uplift of the Khangai Highland and the Mongolian Altai is recorded by the stairs of terraces in the river valleys incising to the mountain slopes. Differentiated vertical movements have been revealed in the near-Baikal part of the Eastern Sayan [67].

Sedimentation continued in the C-shaped belt of basins in the Late Pliocene and Early Pleistocene. Later, the volume of water in lakes changed depending on the alternation of glacials and interglacials. The lake terraces mark the transgressive phases of the water level. The fact that in all basins, the Middle Pleistocene terraces are higher than the Late Pleistocene ones, and the latter are higher than the recent water level, indicates the involvement of the basins to the general uplift of the region.

The increasing contrast of vertical movements is expressed by the coarsening of clastic material. In the Baikal rift zone, the subsidence continues and becomes less and less compensated by sediments with time. Only 300–500 m have accumulated in the South and Central Basins of Baikal, while the thickness of sediments reaches 2 km in the newly formed Northern Basin. In Western Transbaikalia, the subsidence of grabens that arose at the second stage of development continues, and en echelon row of basins is formed in the eastern continuation of the NE end of the Baikal Rift.

A system of active faults in the region has formed in the Late Pliocene–Quaternary, although some elements of this system are inherited from the earlier epochs.

Active Faults

The major active faults in Mongolia and their manifestations during strong earthquakes have been known since the second half of the XX century [3, 5, 14, 53, 55, 59, 70, 79, 84, 91, 105]. In the XXI century, the regime of development of major active faults and the mechanisms of the strongest earthquakes associated with them were studied. These are the Khangai fault with the 23.07.1905 Bolnai earthquake [75, 101, 102], the Ertai fault with the 1931 Fuyun earthquake [88], Dolinoozersky (Bogd) fault with the 1957 Gobi-Altai earthquake [90, 99, 100]. New data have been obtained for the Gurvan-Bulag fault in the Gobi Altai [99], the Erzin-Agardag fault [1], and the faults of the Khubsugul graben [34]. The Kaakhem active fault zone and records of the associated 2011–2012 Tuva earthquakes were identified and studied in the east of Tuva [33]. The detailed studies were carried out in the Tunka-Mondy fault zone, which limits the Tunka system of basins to the north [20, 23, 67, 68], and the most active in the Late Quaternary southeastern part of the Main Sayan Fault [98].

Numerous works were devoted to active faults in the Baikal rift zone, the western and northern Transbaikalia and manifestations of their recent seismic activity [4, 16, 20, 24, 48, 49]. An important contribution to the active fault studies in the region was the

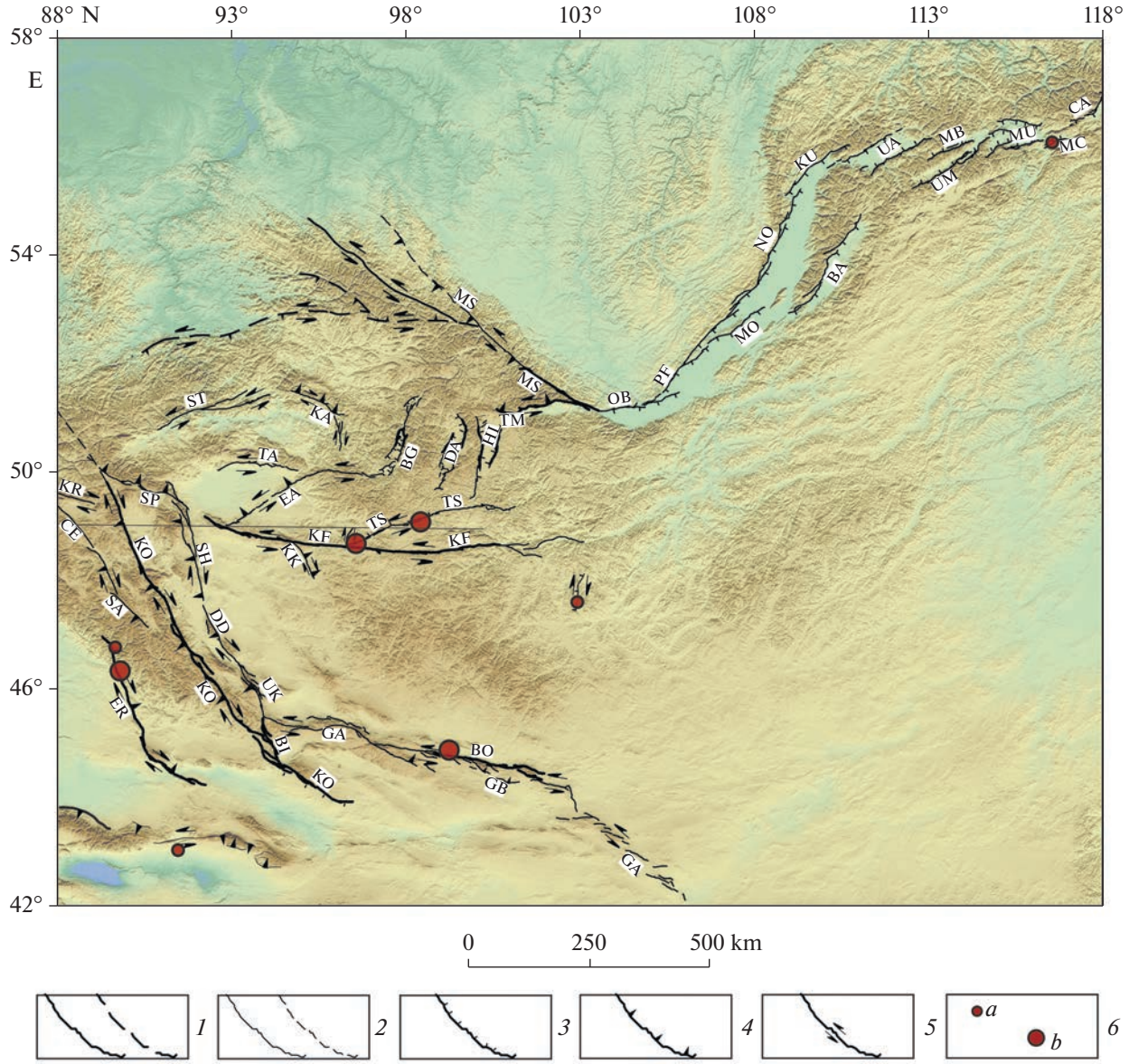

Fig. 7. Major active faults in the northern Central Asia. *Faults*: (BI) Bidj, (BO) Bogd, (CE) Chuya 2003 earthquake rupture, (DD) Dzun-Dgirgalant, (EA) Erzin-Agardag, (ER) Ertai, (GB) Gurvan-Bulag, (KF) Khangai, (KK) Khan-Khukhiyn, (KO) Kobdo, (KR) Kubarda, (KU) Kuchera, (MO) Morskoi, (MS) Main Sayan, (MU) Muya Basin, (NO) North Baikal, (OB) Obruchev, (PF) Primorsky, (SA) Sagsay, (SH) Tsagan-Shibetu, (SP) Shaptal, (ST) Sayan-Tuva, (TA) South Tannu-Ola, (TS) Tsetserleg, (UK) Umusin-Khairkhan; *fault zones*: (BA) Barguzin, (GA) Gobi-Altai, (KA) Kaakhem, (MC) Muya-Chara, (TM) Tunka-Mondy, *grabens*: (BG) Busiyg-Gol, (DA) Darkhat, (HL) Khubsugul, *basins*: (CA) Chara, (MB) Muyakan, (MU) Muya, (UA) Upper Angara, (UM) Upper Muya Basin. *1* – active faults with rates of movements ≥1 mm/year, proved and assumed; *2* – active faults with rates of movements <1 mm/year, proved and assumed; *3* – normal faults; *4* – thrusts and reverse faults; *5* – strike-slip faults; *6* – epicenters of earthquakes with magnitudes M_S = 7–7.9 (a) and ≥8 (b).

compiling of the Database of Active Faults of Eurasia [77] and the Database of faults of the Baikal Region activated in the Pliocene–Quaternary, and seismically induced geological processes in the south of Eastern Siberia and adjacent territories [22].

A summary of the most documented published materials, supplemented by the authors' new data of last years is given below (Fig. 7).

Three NW-trending dextral strike-slip zones with reverse component of movements extend along the Mongolian Altai. In the western zone, the leading role belongs to the Ertai Fault, with which the 1931 Fuyun earthquake is associated. The Holocene, Late Quaternary, and Pliocene–Quaternary displacements show the strike slip rate in the interval 4–18 mm/year, and the recent slip rate that has been estimated by geodetic means is 4–12 mm/year; the vertical component is many times smaller [79, 94, 104].

The Kobdo fault is the main one in the middle fault zone [53, 59]. The strike slip rate on it is estimated at

4–5 mm/year from the Middle Pleistocene and during the Holocene [55]. The fault dips at angles of ∟60°–80° SW, and the reverse component of the displacements (the uplifted SW side) is many times smaller than the strike-slip one in the central and northern parts.

The Kobdo fault is accompanied by the WNW-trending right-lateral Kubadra auxiliary fault, which follows along the northeastern side of the intermontane Chuya-Kurai Basin in the Gorny Altai. The Sagsay fault, which is located to the west of the Kobdo fault, shows the same kinematics, but is less extended and with smaller offsets. The fault that strikes along the southwestern side of the Chuya–Kurai Basin and was activated with dextral displacement during the 2003 Altai earthquake is the northwestern continuation of the Sagsay fault [44]. The Shaptal Thrust extends between the Kobdo Fault and the eastern fault zone [32].

The discontinuous eastern zone is formed by the Tsagan-Shibetu, Dzun-Jirgalant, Umusin-Khairkhan-Nuru, and Bidj Faults. The western sides of them are usually uplifted. The rate of the Holocene strike slip on the Bidj Fault is 2–2.5 mm/year, exceeding the vertical component three times [55].

To the east of the dextral strike-slip faults of the Mongolian Altai, the W–E-trending and WSW–ENE-trending sinistral strike-slip faults and zones of left lateral deformation dominate. The southern Gobi-Altai zone consists of three segments. The 1957 Gobi-Altai earthquake is associated with its 270-km-long eastern Dolinoozersky segment (Bogd Fault). The left lateral slip up to 5 m and, possibly, up to 8 m in some places, with the minor uplift of the southern side occurred during the earthquake [5, 21, 53]. Based on the geomorphological correlation, the strike slip rate was presumably estimated at 6–7 mm/year for the Holocene and 8–9 mm/year for the Holocene and Late Pleistocene [55].

The Bogd and associated faults were studied using the ^{10}Be dating in the area of Orog-Nur Lake and the NW–SE-trending Ih Bogd (height is up to 3957 m) and Baga Bogd (height is up to 3590 m) Ridges. These ridges adjoin the Bogd Fault from the south and are formed by the Late Cenozoic anticlines, the folded form of which is expressed by the basement surface bending. The Artz Bogd Ridge is situated to the east of them. The auxiliary (relative to the Bogd Fault) reverse faults extend along the southwestern slopes of the Ikh Bogd and Baga Bogd Ridges and the northern slope of the Artz Bogd Ridge. Reevaluation the obtained ^{10}Be data showed the left lateral slip rate on the Bogd Fault at ca. 1.5 mm/year and rates of reverse slip in the SW slope of the Ikh Bogd Ridge (Gurvan Bulag Fault) at ca. 0.2 mm/year, in the SW slope of the Baga Bogd Ridge at 0.1 mm/year, and in the northern slope of the Artz Bogd Ridge at 0.13 mm/year [99].

On the southeastern strike of the Gobi-Altai zone, en echelon row of the NE-trending grabens and normal faults, forming the W–E-trending zone of left-lateral deformation extends along the northern boundary of the Ordos to the north of the loop of the Huanghe River [80, 93].

The W–E-trending Khangai fault is more than 500 km long. The strongest ($M \geq 8$) 23.07.1905 Bolnai earthquake occurred in its zone. The 1905 left-lateral displacement of 5–6 m [3] and earlier left-lateral offsets [55] were revealed in the fault zone. The strike slip rate was estimated at 7–8 mm/year for the Late Holocene by summing up the displacements during strong earthquakes dated by the ^{14}C method [53]. Later studies using ^{10}Be dating gave the slip rate of 2.5 mm/year for the longer time interval [99]. The vertical component of movements is smaller and variable, more often the southern side is uplifted. The 75 km long Teregtyin right lateral fault with reverse component is conjugate to the Khangai fault and is characterized by the slip rate of 0.5–0.7 mm/year.

The major ENE-trending auxiliary left-lateral faults adjoin the Khangai Fault from the north. These are the Erzin-Agardag fault with an uplifted northwestern side [1] and the Tsetserleg fault with an uplifted southeastern side [55]. The ratio of the coeval Late Holocene strike-slip and vertical components of displacement on the Erzin-Agardag fault is 4–5/1. Our trenching in the northeastern segment of the fault revealed the flower structure characteristic of strike-slip faults and records of as minimum three paleoearthquakes. The 09.07.1905 earthquake ($M = 7.6$) occurred in the Tsetserleg fault zone. The trenching shows records of this and as minimum one previous earthquakes.

The ENE-trending left lateral faults with reverse component are also found in Tuva. The South Tannu-Ola fault cuts the boundary of the Ubsu-Nur Basin and the Tannu-Ola Ridge. The Sayan-Tuva fault borders the Tuva Basin to the north.

The N–S-trending Busiyngol, Darkhat, and Khubsugul grabens that are bounded by normal faults with the Late Quaternary offsets are situated in the northeastern continuation of the Erzin-Agardag fault. The latter merges with the southern end of the Busiyngol graben. The northeastern part of the Tsetserleg Fault joins with the southern continuation of the Khubsugul faults. These grabens form the zone of left lateral deformation that joins the Erzin-Agardag Fault with the Tunka-Mondy left-lateral fault zone, with which the Khubsugul graben merges in the north. The NNW-trending Kaakhem right-lateral zone with reverse component [33] limits the left-lateral faults of Tuva from the east and adjoins the Busiingol graben in the south.

The W–E-trending Tunka-Mondy left-lateral fault zone with reverse component of movements limits the chain of the Tunka basins to the north. In the western part of the zone (the Mondy Fault), the strike slip rate is 1.1 mm/year and the reverse compo-

nent rate is 1 mm/year [68]. In the more eastern Tunka part of the fault zone, the strike-slip rate is 1.5 mm/year with a vertical component of movements of ca. 1 mm/year [67]. The Tunka-Mondy zone is adjacent in the east to the most active southeastern part of the Main Sayan Fault with the strike-slip rate of 1.4 ± 0.1 mm/year [98]. The increased Late Quaternary strike slip rate in the southeastern part of the Main Sayan Fault weakens to the NW and is transferred to the Tunka-Mondy fault zone.

The Baikal rift zone extends to the NE from the southeastern part of the Main Sayan fault. The major faults strike along the northwestern side of the rift and are expressed by steep scarps. They are (from south to north): Obruchev, Primorsky, North Baikal, and Kuchera Faults. The Morskoy Fault branches off from the Primorsky Fault and continues along the southeastern slope of the Olkhon Island and the Akademichesky Ridge, limiting the Central Basin of Baikal. Near the land surface, the dips of faults are ∟60°–70° to the SE, but arguments are given that the Primorsky fault is listric [4].

The rate of vertical movement is estimated on the Primorsky Fault at 0.9 ± 0.2 mm/year during the last 2500 years [66] and on the Kuchera Fault at 0.2 (up to 0.4) mm/year during the Late and Middle Pleistocene [69]. The faults on the southeastern coast of the Baikal Lake are less extensive and often arcuate. Some of them show a listric structure. If the listric structure of the faults is taken into account, these estimates are consistent with the GPS measurement data, which show the rate of extension of the Olkhon block between the Primorsky and Morskoy Faults at 1–1.5 mm/year [48] and the rate of extension of the entire Baikal rift zone at 4 mm/year [74].

The rate of vertical movements reaches 0.2 mm/year on the Barguzin normal fault zone, limiting the Barguzin Basin to the NW [2, 97]. En echelon row of the NE-trending graben-like basins extends to the west of the northeastern end of the Baikal rift zone. The structure of basins is controlled by longitudinal normal faults, sometimes with smaller left lateral component [4, 24]. The Muya-Chara fault extends along the axis of en echelon row of the basins. The left-lateral component of movements on the fault is commensurable with the normal one. This zone of left-lateral deformation continues to the east, into the Stanovoi Ridge, by the W–E-trending left-lateral faults with reverse component of movements [13].

Thus, the described active faults form a single structural ensemble. It is represented in the western and central parts of the region by a combination of the NNW-trending right-lateral faults with reverse component of the Mongolian Altai and the Kaakhem zone and the W–E-trending and WSW– ENE-trending left-lateral faults that often have the reverse component also. The N–S-trending normal faults of the Busiyngol, Darkhat, and Khubsugul grabens are situated in continuation of strike-slip faults and play the same kinematic role. In the Baikal rift zone and Transbaikalia, the NE-trending normal faults dominate. They are partly grouped into the W–E-trending zones of left-lateral deformation. Thus, the entire ensemble of active faults has been formed under conditions of NE–SW compression and NW–SE extension. The transpression dominates in the western and central parts of the region, while transtension and extension dominate in the NE [54, 95]. An analysis of the mechanisms of earthquake sources confirms this assessment [29, 47, 93].

A summing of the results of GPS measurements shows a change in the direction of movement of crustal blocks from the NE under conditions of transpression in the west and in the center of the region to the SE under conditions of transtension and extension in the east [25, 46, 73, 74, 96, 110, 111]. The cited authors attribute this change to a combination of the influence of the Indo-Eurasian collision, which dominates in the west and center of the region, and the Pacific subduction, which caused the Amur Plate movement away from the Siberian Platform.

THE KHANGAI INTRAMANTLE PLUME

Zorin et al. [11, 12, 81, 115] showed the lithosphere is thinned in the region of the Khangai Highland, its northern slope near the Khubsugul Lake, and Western Transbaikalia due to the supposed impact of the anomalous (heated and decompressed) upper mantle located below. Seismological studies suggested the presence of a mantle plume (or plumes) in the mantle of this region [15, 85], but the contours and depth of the revealed volumes of the low-velocity mantle have not been determined in details.

Based on an analysis of the δVp model MITP08, we determined the outlines of the Khangai plume and showed that it rises from depths of ca. 1250 km [56]. Huang and Zhao [86] proposed the different Khangai plume model based mainly on data from local seismic stations. According to this model, the low-velocity volume is located under the highest southern part of the Khangai Highland and is surrounded by a high-velocity ring that includes topographic depressions around the highland and may be a blurred image of local mantle heterogeneities. The ring is surrounded by relatively low-velocity volumes of the crust and mantle under the Altai, the Sayans, a part of Baikal and the Khentei Highland. The Khangai low-velocity body is traced to depths of ca. 120 km. Below, it is replaced by a high-velocity mantle, which is replaced by a low-velocity mantle deeper than 300 km, the top of the latter being somewhat south of the upper low-velocity volume.

An analysis of Late Mesozoic and Cenozoic intraplate basaltic volcanism led to the assumption that it is partly due to upper mantle plumes [62, 112, 113].

According to Yarmolyuk et al. [62], these plumes rise from the proposed volume of heated matter at the lowest mantle. Below we present new data that refine the contours of the plume and characterize its structure.

A series of horizontal slices of the mantle constructed on the basis of the MITP08 model shows that under the territory of Mongolia and Western Transbaikalia, the upper mantle above its transitional layer is a vast "hot" (low-velocity) field that continues to the Central and Eastern Tibet (Fig. 8). The slices show that this field has the most negative velocities in the area that we identified earlier as the Khangai plume [56]. "Hot" values in the territory of Mongolia have almost the same intensity as the flows of SE Asia, which are branches of the Pacific superplume. At the sublithosphere depth of 112 km (Fig. 8), the Khangai and Tibetan plumes are separated by a narrow partition. Below, at a depth of 419 km, vertical "hot" cavities alternate with less negative volumes.

At a depth of 655 km, a narrow western branch of the low-velocity field approaches the eastern continuation of the African plume branch, but the connection between them is interrupted by the high-velocity Neotethys slab. The "hot" part of the Khangai plume is shifted to the SE at the level of the transitional mantle layer compared to the "hottest" part of the plume in the upper mantle. At a depth of 1016 km, the intensity of velocity variations decreases, and possible connections of the Khangai and Tibetan plumes with branches of the Pacific plume, the N-trending between 102° and 109° E and the W-trending between 42° and 43° N, are revealed.

The 3D visualization of the tomographic model (Fig. 9) shows two pairs of orthogonal (N–S-trending and W–E-trending) sections of the mantle viewed from the SE. The junction of the sections of the western pair is located under the Southern Urals (ca. 54° N; 60° E). Here, at the base of the both sections, i.e., above the mantle-core boundary, a volume is distinguished with significant negative δVp, close in their values to low-velocity volumes at the base of the African and Pacific superplumes. Preliminary analysis of the MITP08 model shows that this volume continues under the eastern part of the East European Platform.

This object is not an artifact of the calculation method used by the authors of the MITP08 model [92]. Bono et al. [72] provides an overview of the configuration of superplume roots above the mantle-core boundary for five different models of velocity variations, from which it follows that a small superplume root under the East European Platform is confidently distinguished by different authors, but its root area is significantly smaller than those of the African and Pacific superplumes. The low-velocity volume identified by us at the base of the mantle continues upward as a discontinuous chain of volumes with negative δVp, which are associated with the upper mantle volume located slightly to the south (the maximum is between 40° and 45° N) with significant negative δVp (Fig. 4a), contoured by an isosurface of –0.22% (Fig. 4b). This volume is separated by a neck from the low-velocity upper-mantle branch of the African superplume in Iran south of 35° N. Such a pattern of mantle velocity anomalies allows for a connection between the upper mantle low velocity volume located in the north of the N-trending section, both with the African superplume or with the low velocity local volume at the base of the mantle. The more detailed analysis of the latter goes far beyond the scope of our paper.

The junction of the sections of the eastern pair falls on the northern limit of the Khangai plume in Tuva (ca. 54° N; 96° E). The N–S-trending section of this pair (Fig. 9a) shows the Khangai plume, which, narrowing down, is traced to a depth of ca. 1270 km. The same section shows low-velocity volumes of the upper mantle and uppermost lower mantle beneath Central Tibet and Myanma. The W–E-trending section shows the possibility of a connection between the Khangai plume and relatively low-velocity volumes of the upper mantle of Northern Transbaikalia in the sublithosphere level and at depths of 700–1000 km.

The structure of the lower boundary of low-velocity volumes represented by the –0.22% isosurface (Fig. 9b) shows that the Khangai plume is connected with the Tibetan plume and low-velocity volumes of Transbaikalia in the upper part of the lower mantle at depths of up to 1000–1200 km. The southern deep branch of the combined plumes may have a communication channel with the western branch of the Pacific superplume located at depths of 1300–1600 km.

Two orthogonal sections of the mantle viewed from the NW are represented in Fig. 10. The junction of the sections is located under Eastern Mongolia (ca. 48° N; 108° E).

The W–E-trending section crosses the main body of the Khangai plume under the southern Khangai Highland. The plume is of the biggest width and is characterized by the lowest δVp values in the upper mantle. The reduction of seismic velocities decreases in the transition layer of the mantle and increases again in the upper part of the lower mantle (800–1200 km) under the eastern part of the plume. The plume root is located at the depth of 1300 km. The smaller body with the negative δVp is identified SE of the Hentei Highland and is seen in the N–S-trending section. It is isolated from the main body of the Khangai plume in depths up to 700 km, but they are connected below, in the uppermost lower mantle.

So, the Hentei body is a branch of the Khangai plume. The areas with weakly reduced δVp can be interpreted as possible channels of connection of the Khangai plime with distant branches of the superplumes. These are the possible channels of connection with the northeastern branch of the African superplume at the level of the transitional layer and the uppermost lower mantle and with the western branch

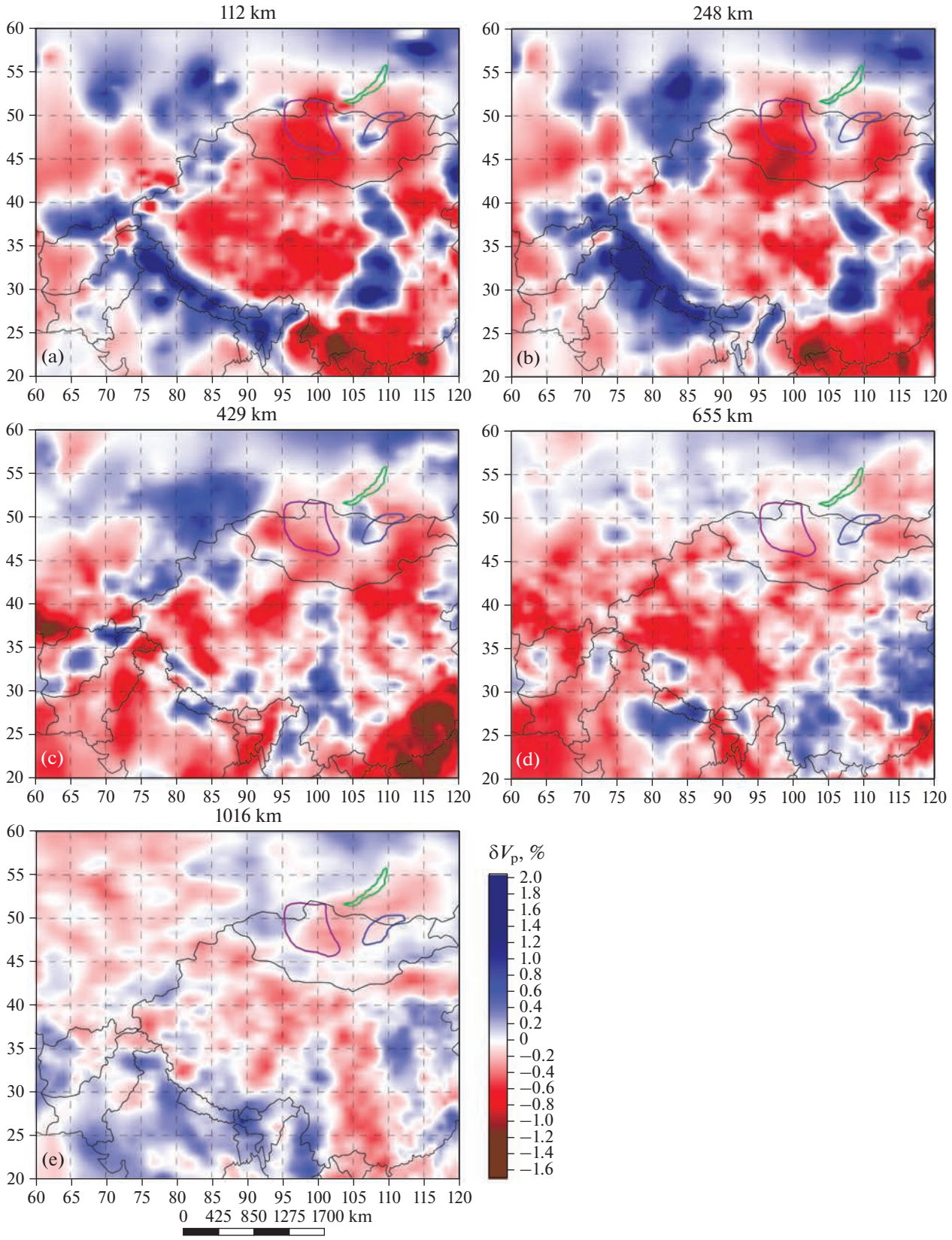

Fig. 8. Variations of seismic velocities δVp in the region of the Khangai and Tibetan plumes and their surrounding, based on the MITP08 model [92], in different horizontal slices of the mantle: (a) – 112 km; (b) – 248 km; (c) – 665 km; (d) – 1016 km.

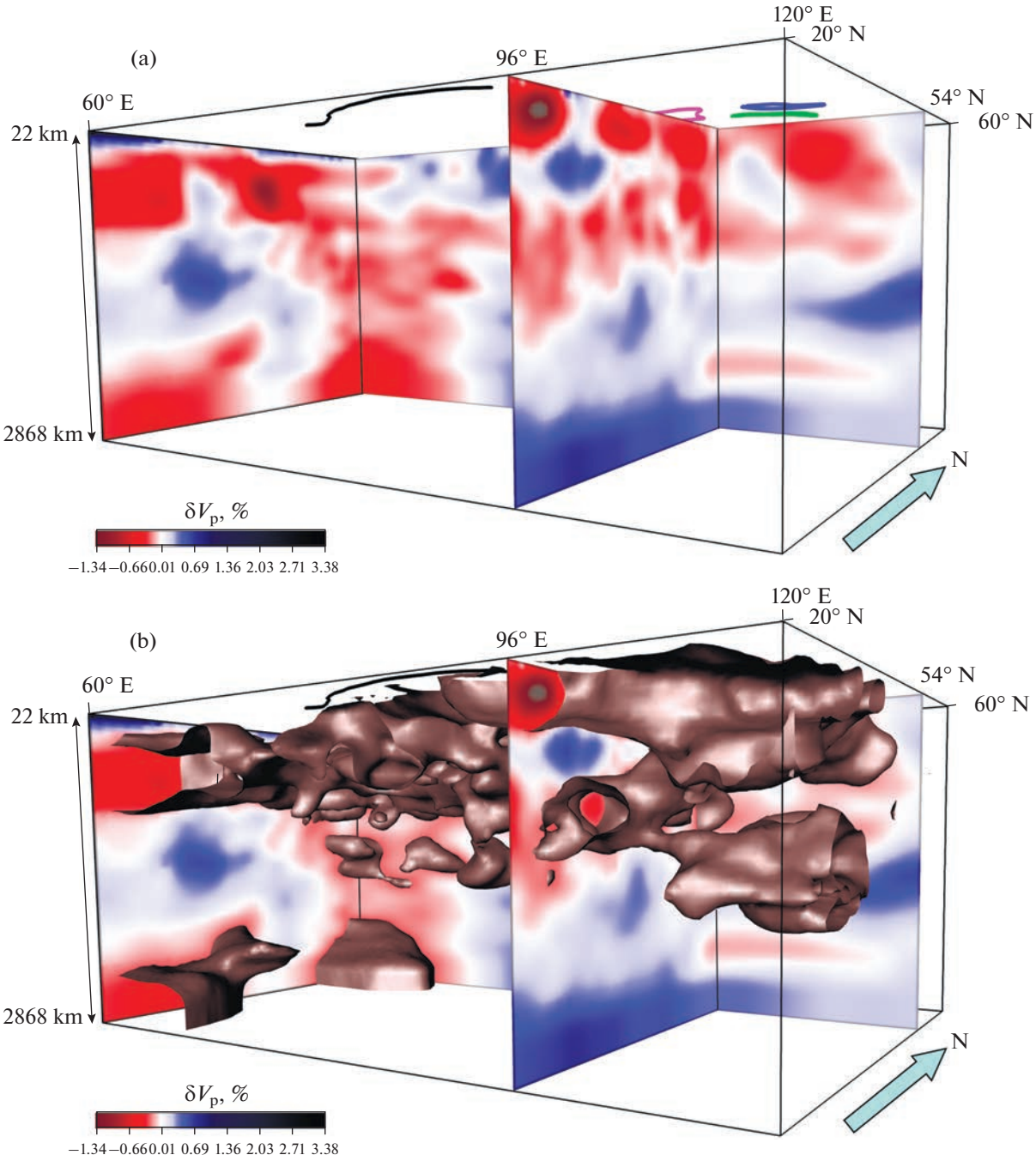

Fig. 9. Volumetric distribution of variations of seismic velocities δ*Vp* in the region of studies, based on the MITP08 model [92]: (a) – the W–E-trending and the N–S-trending δ*Vp* sections: (b) – the same with isosurface –0.22%. Two orthogonal intersections of the sections (vertical planes) and southern flank of the Himalayas (black line) are shown. The horizontal contour of volumetric block corresponds to fig. 1. A point of observation is in the SE and a direction of observation is oriented from the depth to the surface. Two pairs of the orthogonal sections are shown. The sections of the western pair (coordinates of their junction are 54° N and 60° E) extend along the western boundary of the region and near the northern boundary of the region. The sections of the eastern pair (coordinates of their junction are 54° N and 96° E) strike across the Tibetan and Khangai plumes, Baikal Lake and Transbaikalia.

of the Pacific superplume in the lower mantle. The channels have a small negative level of velocity variations, which does not go beyond –0.22%. In this regard, the continuity of their tracing is lost in Fig. 10b.

The other pair of orthogonal sections of the mantle viewed from the NW is shown in Fig. 11a. The junction of the sections is located under the eastern edge of Tibet (ca. 31° N; 103° E).

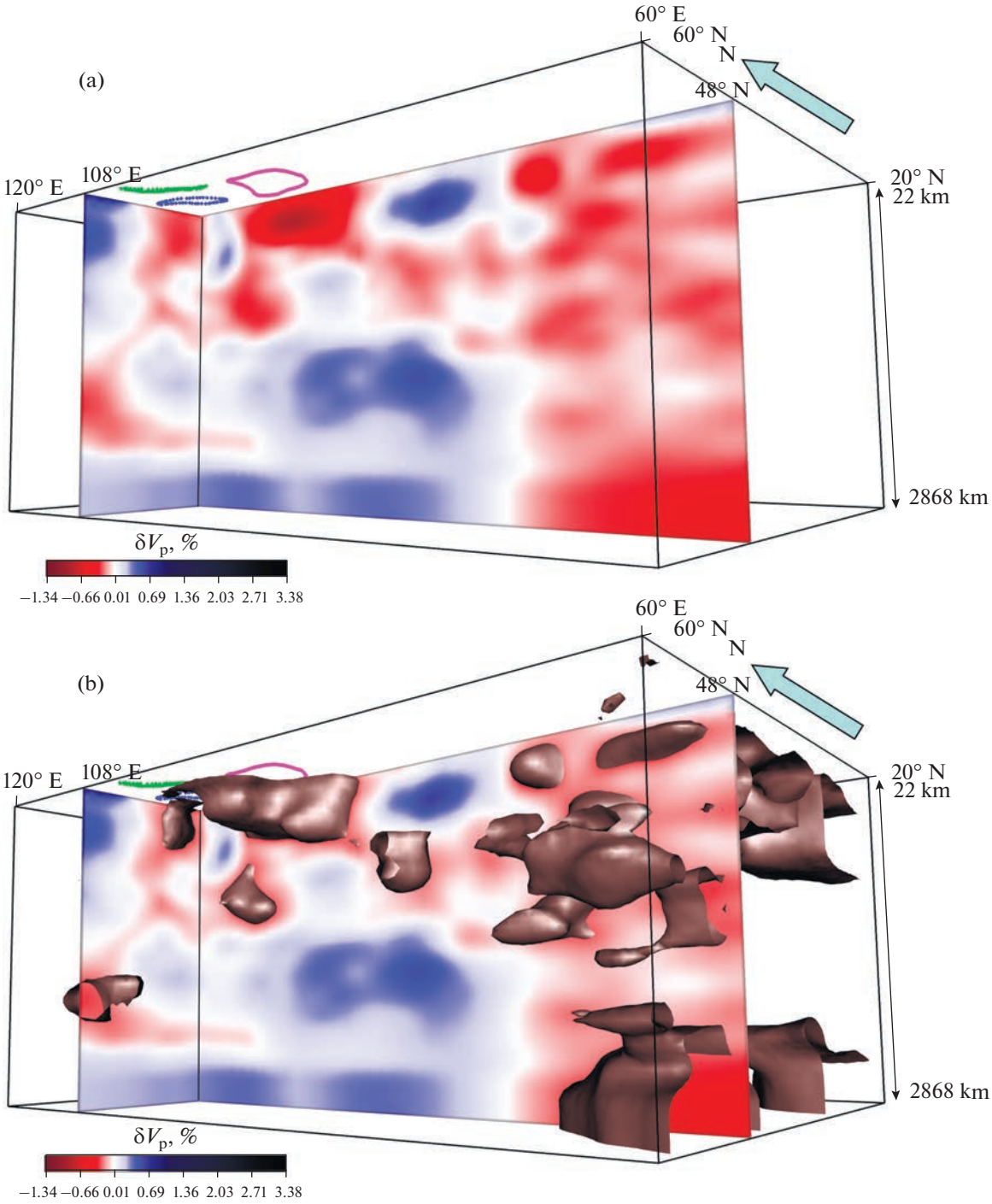

Fig. 10. Volumetric distribution of variations of seismic velocities δ*Vp* in the region of studies, based on the MITP08 model [92]: (a) – the W–E-trending and the N–S-trending δ*Vp* sections: (b) – the same with isosurface –0.22%. The horizontal contour of volumetric block corresponds to Fig. 1. A point of observation is in the NW and a direction of observation is oriented from the depth to the surface. The W–E-trending section demonstrates the main body of the Khangai plume, and its Khentei branch and the low velocity volumes of Transbaikalia are shown in the N–S-trending section.

The N–S-trending section crosses the eastern part of the Khangai plume. At the upper mantle level, its branch is observed, following to the NE to Transbaikalia. At the level of the transitional layer of the mantle, the intensity of the δ*Vp* variations weakens. Below it increases, and the plume reaches a depth of 1250 km. The Khangai plume is separated from the Tibetan plume by a narrow bar. In the W–E-trending section, the Tibetan plume has the shape of an overturned cone, the top of which is at a depth of ca. 1530 km. In the upper mantle part, the

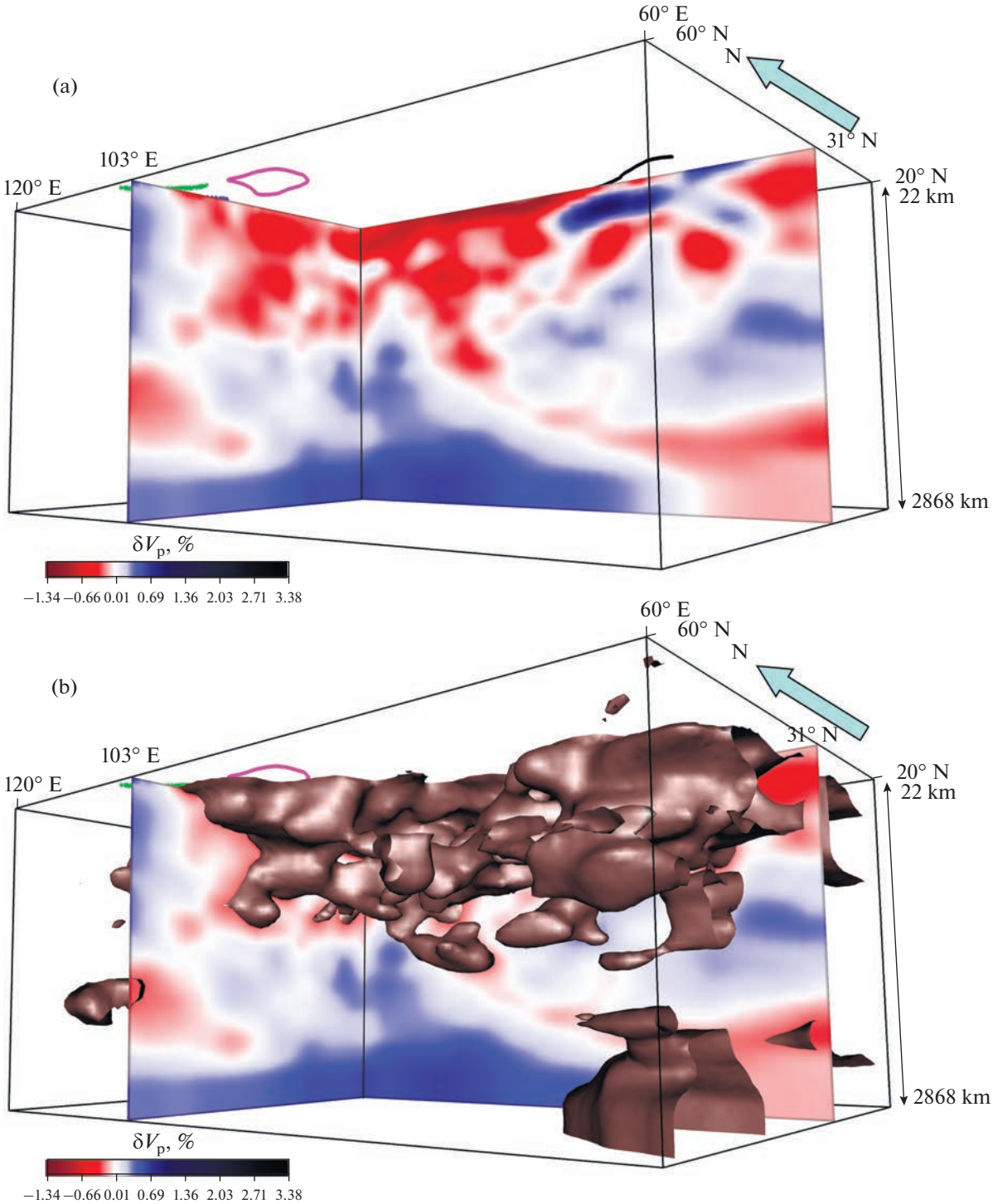

Fig. 11. Volumetric distribution of variations of seismic velocities δ*Vp* in the region of studies, based on the MITP08 model [92]: (a) – the W–E-trending and the N–S-trending δ*Vp* sections: (b) – the same with isosurface –0.22%. The horizontal contour of volumetric block corresponds to Fig. 1. A point of observation is in the NW and a direction of observation is oriented from the depth to the surface. The W–E-trending section demonstrates the Tibetan plume, and the Khangai plume is shown in the N–S-trending section.

Tibetan plume, like the Khangai plume, is characterized by sharply negative δ*Vp*. At the level of the transitional layer of the mantle, the plume is divided into separate ascending jets, which merge into one at the uppermost lower mantle. Below, the size of the plume is reduced. Above both plumes, the lithosphere is thinned.

The uneven lower boundary of the Khangai and Tibetan plumes and its sharp depressions, marking the

places of plume roots, are visible in Fig. 11b. The figure also demonstrates possible channels of connection between the Tibetan plume and the low-velocity volumes of the upper mantle and uppermost lower mantle under the southern part of the Turanian Plate, probably representing the branch of the African superplume.

The structural details of the Tibetan plume, which largely coincide with those observed in Fig. 11a are visible in Fig. 12a, where the orthogonal sections converge under Tibet (ca. 33° N; 86° E) and viewed from the NE. The plume has the shape of an overturned cone with a peak at a depth of 1400–1500 km. The cone is horizontally stratified. The upper "hot" layer is located between the base of the thinned lithosphere (ca. 50 km) and the top of the transitional mantle layer (ca. 400 km). Below, from ca. 400 to ca. 1000 km, horizontal lenticular "hot" volumes alternate with higher velocity volumes. Deeper, the area of "hot" volumes is reduced, and their velocity contrast with the surrounding mantle decreases.

When visualizing a tomographic model bounded by an isosurface of negative deviations of –0.22% (Fig. 12b), a chain of "hot" cavities connected together is visible between the orthogonal sections, rising from the depth and flowing into the upper "hot" layers. In the foreground, the Khangai plume and its branch, which is located immediately to the south and east of the Khentei Highland and is connected with the Khangai plume at depths of up to 900–1000 km, are visible. At the same time, the Khentei branch has its own small root reaching depths of 1000–1100 km. The main body of the Khangai plume is located under the territory from the Gobi Altai in the south to the southern foothills of the Eastern Sayan in the north. The plume reaches its greatest depth (ca. 1300 km) under its southern part. The "hot" anomaly extends from it to the southern Transbaikalia, but is replaced by "cold" volumes under Baikal itself.

Thus, the orthogonal sections of the Central Asian mantle (Figs. 9–12) demonstrate the complicated structure of the Khangai and Tibetan plumes. The main body of the Khangai plume, expanding upward, rises from a depth of 1300 km. The Khentei plume separates from it at the uppermost lower mantle level (ca. 800–1000 km). The low-velocity branches of the main Khangai plume and its Khentei part propagate to Transbaikalia. There are chains of cavities with weakly reduced δVp, which can be interpreted as connecting channels of the Khangai and Tibetan plumes with distant branches of the African and Pacific superplumes.

DISCUSSION

Structural Parageneses

Structural paragenesis is an ensemble of interconnected tectonic forms of folding and/or faulting united by a common origin [21]. We distinguish two structural parageneses in the Cenozoic structure of the studied region. Tectonic forms either entirely belong to one of them, or are an integral effect of the interaction of processes responsible for their development.

The first structural paragenesis is represented by active faults created by the action of horizontal NE–SW compression and NW–SE extension. The strike-slip faults dominate (Fig. 7). In the west of the region, they usually have a reverse displacement component, which indicates transpression, and in the east they are accompanied or replaced by extensional grabens, which are oriented to the NE, obliquely with respect to the direction of left-lateral deformation. The boundary between the compressed and stretchable parts of the region runs along approximately 105° E. The significance of this border was noted decades ago by Chinese scientists [17, 79].

The second structural paragenesis (let's call it "Khangai") unites the arched uplifts of the Khangai and Khentei Highlands, C-shaped belt of basins around the Khangai Highland, and the belt of depressions in the southeastern Mongolia (Fig. 13). There are no signs of the influence of the system of horizontal stresses, which control the first paragenesis, on the formation of the second paragenesis. It is caused by the vertical pressure responsible for the formation of the arches, and the radial forces around the Khangai arch, which caused the subsidence of basins.

The geodynamic processes that created the both structural parageneses are combined in the Late Pliocene and Quaternary with the total uplift of the region. The basins of the C-shaped belt have been involved in the uplift since the Middle Pleistocene.

The geodynamic sources and the tectonic stress fields, which are responsible for the listed tectonic phenomena, are different. The Late Cenozoic uplift of mountainous systems is the global phenomenon. Active faults of the first paragenesis are widespread throughout the study region and continue to the neighboring parts of the Alpine-Himalayan and Altai-Stanovoy mountain belts. Structural manifestations of the "Khangai" paragenesis are concentrated in the central part of the study region.

The combination of geodynamic influences, responsible for the formation of two structural parageneses, on the same territory can be explained by two ways:

— the parageneses are of different age;

— the parageneses reflect tectonic processes occurring at different levels of the tectonosphere.

Active faults are the Late Quaternary by definition [64, 107]. Data have been obtained that displacements on some active faults, similar to the Late Quaternary ones, occurred during the whole Pleistocene and even the end of the Pliocene [22]. The Khangai and Khentei Highlands steadily rose and served as sources of detrital material from the Late Jurassic [2], while the basins of the C-shaped belt developed most intensively during the accumulation of the middle tectonic-strati-

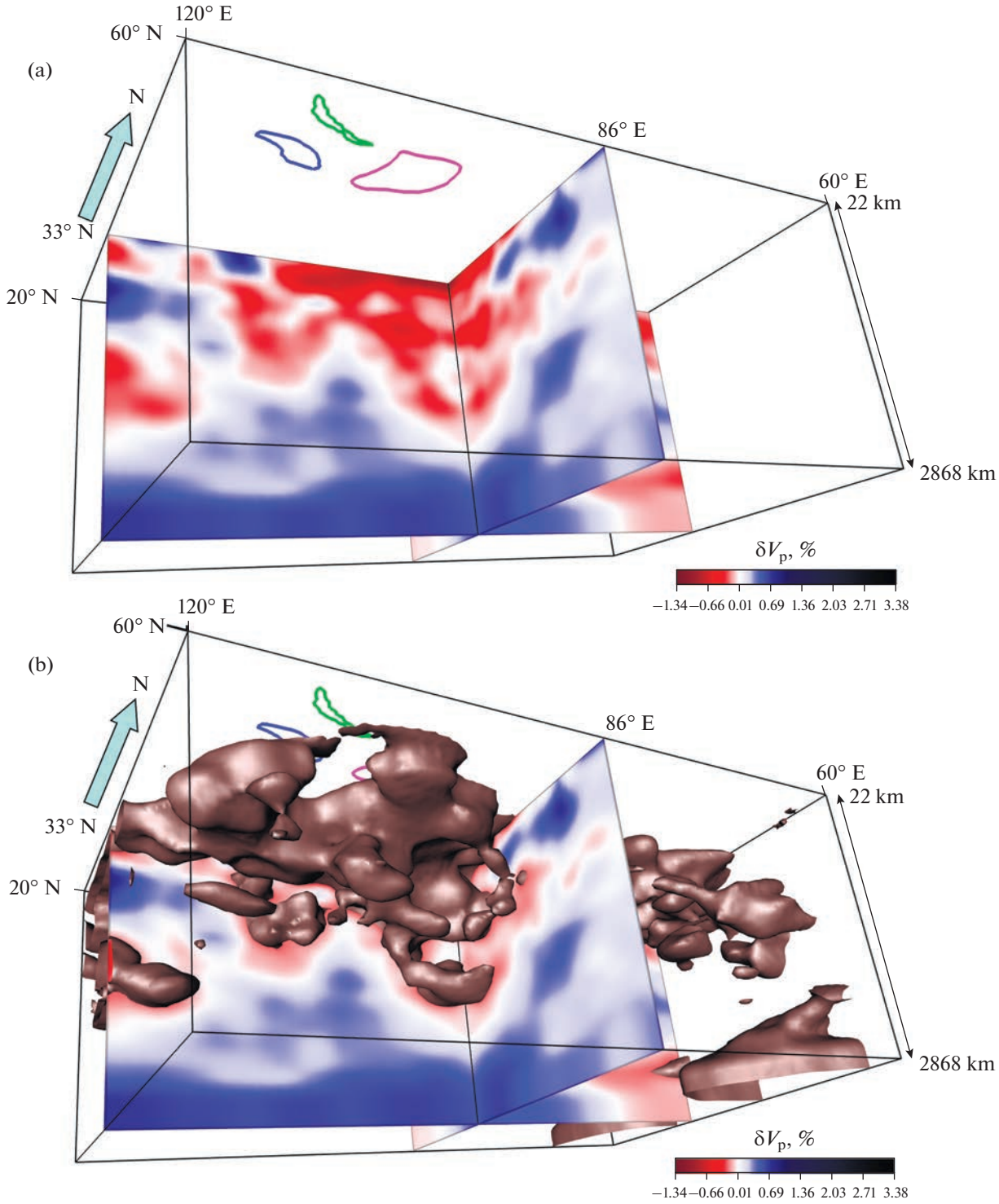

Fig. 12. Volumetric distribution of variations of seismic velocities δ*Vp* in the region of studies, based on the MITP08 model [92]: (a) – the W–E-trending and the N–S-trending δ*Vp* sections: (b) – the same with isosurface –0.22%. The horizontal contour of volumetric block corresponds to Fig. 1. A point of observation is in the NE and a direction of observation is oriented from the depth to the surface. Figure a demonstrates the Tibetan plume, and a root of the Khangai plume is seen in Figure b.

graphic group (Late Oligocene–Early Pliocene). It would seem that the second paragenesis is older than the first, but this assumption turned out to be wrong.

We do not have data on the strike-slip movements on active faults earlier than the Late Pliocene–Quaternary, except for Deviatkin's [7] suggestion of the

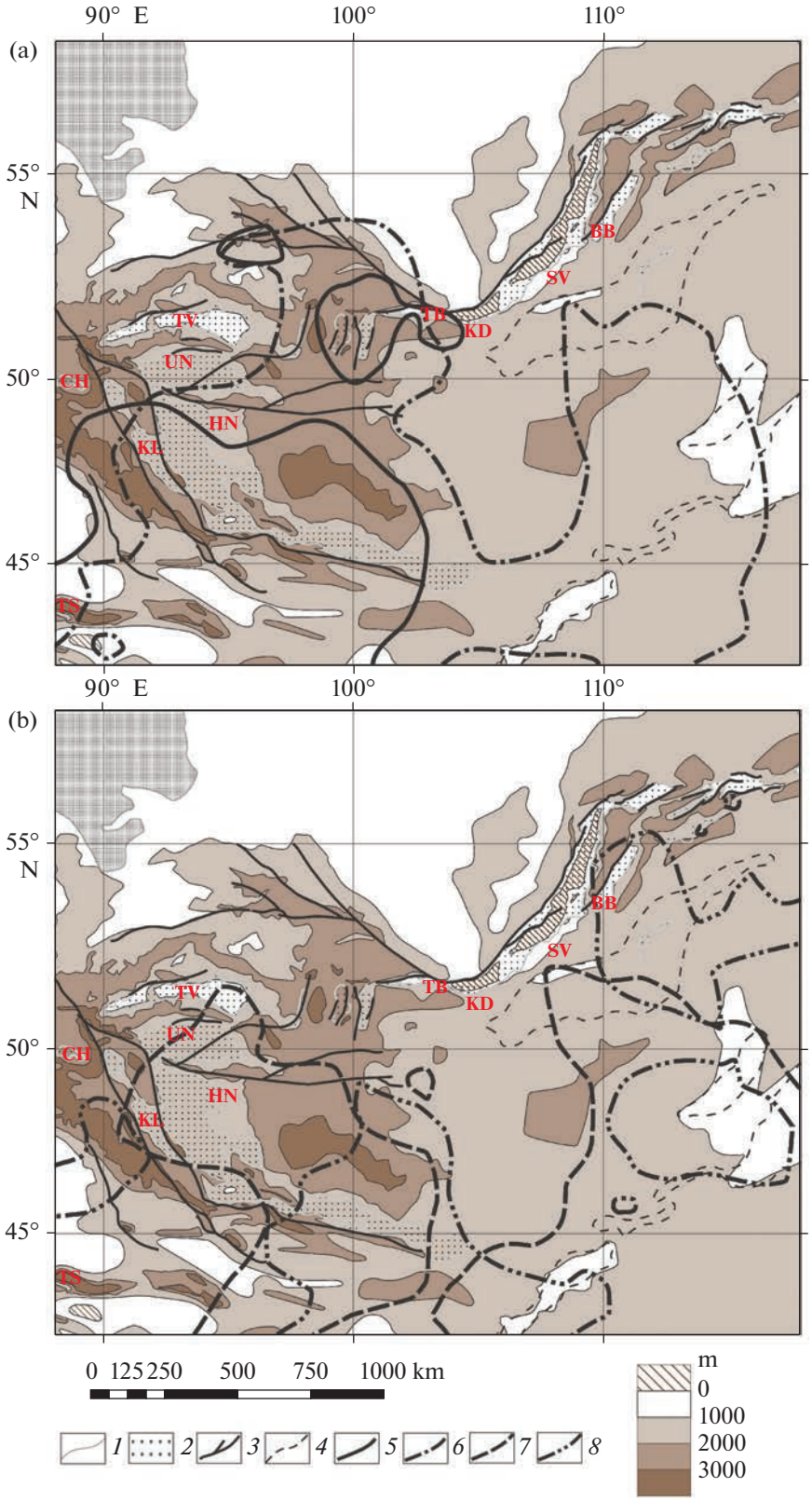

Fig. 13. Correlation of the structural paragenesis of the Khangai and Khentei arches and surrounding basins and contours of the Khangai plume in different depths of the mantle by the isosurface –0.22%. The contours of the plume are shown for the depths of 67 and 248 km (a) and 384 and 655 km (b). *Basins*: (BB) Barguzin, (KD) South Baikal, (KL) Depression of Big Lakes, (SV) Central Baikal, (TB) Tunka, (TV) Tuva, (UN) Ubsu-Nur: *ridges*: (HH) Khan-Khukhein, (TS) Tien Shan. *1* – isolines of a summit plane of the basement in uplifts and a bottom of sedimentary cover in the basins; *2* – deposits of the Late Mesozoic and Cenozoic basins and grabens; *3* – major faults; *4* – contours of troughs, Selenga-Vitim and of Eastern Mongolia; *5–8* – contours of the Khangai plume at the depths of: *5* – 67 km, *6* – 248 km, *7* – 384 km, *8* – 655 km.

post-Middle Jurassic 70 km right-lateral offset on the Tsagan-Shibetu Fault. However, it is possible to estimate the age of other Cenozoic structural elements similar to those elements of the active fault paragenesis that accompany strike-slip faults. The Late Quaternary normal fault displacements in the Baikal rift zone and Transbaikalia inherit similar earlier displacements. The Southern and Central Basins of Baikal have been developing since the Eocene, and possibly the Late Cretaceous. The NE-trending grabens of Transbaikalia formed from the Late Cretaceous throughout the entire Cenozoic; they were preceded by graben-like basins like the Gusinoozerskaya and Tugnui, which arose in the Jurassic and Early Cretaceous [2]. Thus, the development of the en echelon row of the NE-trending grabens as a manifestation of W–S-trending left-lateral strike-slip deformation took place in the Baikal region and Transbaikalia simultaneously with the growth of the Khangai and Khentei arches.

The Gobi Altai, the Mongolian Altai, and the Eastern Sayan are the outer frame of the basins of the C-shaped belt and can be interpreted in two ways. It can be assumed that their rise was, at least partly, a distant result of the influence of radial forces caused by the Khangai arch uplift. The fault outer boundaries of the C-shaped belt testify to this influence.

Cases of intersection of active faults and structural boundaries of the C-shaped belt basins are revealed. For example, the Erzin-Agardag and South Tannu-Ola active left-lateral faults with reverse component cut obliquely the boundary of the Tannu-Ola Ridge and the Ubsu-Nur Basin. The paper [67] reports kinematic changes during the development of the Tunka-Mondy fault zone. Since the Middle Pleistocene, the zone has been developing as an active left-lateral fault with reverse component, but it shows signs of left-lateral movements with normal component at the earlier stages, when the Tunka Basin developed as a part of the C-shaped belt. These data testify in favor of geodynamic differences between the two parageneses and the connection of the linear mountain uplifts with the "Khangai" paragenesis.

However, a lot of data indicate the similarity of the geodynamic conditions for formation of the paragenesis of active faults and mountain uplifts in the outer framing of the C-shaped belt of basins. The transpressive nature of the Late Cenozoic deformation in the Goby Altai is reported [76]. The bending deformation of the basement surface testifies to the compression or transpression during the formation of the Gobi Altai and Mongolian Altai, starting from the Late Oligocene. The Kobdo active right-lateral fault with reverse component plays a structure-forming role in the Mongolian Altai. The Late Cenozoic compression in the Eastern Sayan [2] and the presence of a reverse displacement component on the long developed Main Sayan Fault [4] were substantiated.

The compression component is also expressed in the ridges separating the basins of the C-shaped belt. It is reported about the thrusting of the basement on the Jurassic deposits and the Jurassic deposits on the Pliocene–Quaternary in the southern slope of the Khan-Khukhein Ridge [7]. The compression is expressed by near-fault folding of the Miocene–Lower Pliocene deposits in the southern slope of the Tannu-Ola Ridge. So, the formation of the structure of the mountain ranges of the outer frame of the C-shaped belt of basins and the bridges between the basins of the belt occurred from the late Oligocene in the same geodynamic regime as the paragenesis of active faults. Therefore, the elements of the structural paragenesis, expressed by active faults, developed for a long time and simultaneously with the "Khangai" paragenesis, i.e., the differences in their origin are related to the impact of processes occurring at different depths of the tectonosphere.

Correlation of the Mantle Irregularities and the Cenozoic Structure in the Region

An analysis of the 3D distribution of velocity variations in orthogonal sections, the junction of which is focused in the Khangai plume, shows that at depths of 800–1000 km there is a communication channel between the main body of the Khangai plume and the Khentei anomaly (Fig. 10a). They can be considered as a single complex Khangai plume, although each of these volumes is a separate "hot" cavity, distinguished by the –0.22% isosurface. It is shown that the low-velocity flows penetrate into Transbaikalia either from the main body of the Khangai plume or from its Khentei branch (Fig. 8).

Several horizontal slices of the mantle demonstrate changes in the shape of low-velocity volumes of the Khangai plume and Transbaikalia, limited by the –0.22% isosurface (Fig. 13).

The slice at a depth of 248 km, located in the middle between the base of the lithosphere (50–100 km) and the top of the transitional mantle layer (ca. 400 km), shows the maximum distribution of the "hot" mantle under the Khangai Highland and the Gobi Altai, as well as under the eastern part of the Khentei Highland and the area to the south and east of it. The Khangai "hot" volume reaches Tuva and the Eastern Sayan in the north, and the Khentei hot volume reaches Southern Transbaikalia, but they do not capture Baikal and the depression of the Selenga River basin. The bodies of the low-velocity mantle of the Khangai plume and its Khengei branch are interconnected in the south and continue towards the Tibetan plume, indicating the communication of heated sublithospheric masses between them. The more compact low-velocity volumes, which are contoured at a depth of 67 km, extend upwards from the unified Khangai-Khentei "hot" body. They cover Eastern Tuva, the southern foothills of the Eastern Sayan and the neighboring part of

Mongolia, the Gobi Altai and the southeastern Mongolian Altai.

At a depth of 384 km, the Khangai-Khentei "hot" body splits into the western Khangai and eastern Khentei parts (Fig. 13), maintaining a connection at a greater depth (Figs. 10a and 11a). The Khangai part covers only the southern Khangai Highland and the Gobi Altai. The possibility of connection with the Tibetan plume becomes more obvious. At a depth of 655 km, the contour of the Khangai plume decreases and shifts to the SE towards Tibet. The Khentei anomaly persists as an isolated spot. Another low-velocity area is located under Transbaikalia. Narrowing, it continues to the east, which indicates its possible connection with the Pacific active margin. To the north of the Transbaikalia "hot" area, several small hot spots are distinguished. Communication between the Khangai plume and the low-velocity mantle of Transbaikalia is restored at depths of ca. 1000 km (Fig. 9a). At the 1016 km dip slice, the intensity of the decrease in *P*-wave velocities weakens (Fig. 8). The Khangai plume is displaced to the east relative to its position in the upper mantle. The root part of the plume is connected by a corridor of weakly reduced *P*-wave velocities with the low-velocity volume of Transbaikalia.

Thus, the body of low-velocity mantle of the Khangai plume is traced from depths of ca. 1300 km. The plume widens upward, and the greatest decrease in velocities is found at depths of 100–400 km. Above the plume, the lithosphere is heated and thinned up to 50 km. The plume forms the Khentei branch in the south and is connected with low-velocity volumes of the mantle of Transbaikalia in the north. The contours of the Khangai plume cover the area of manifestation of the "Khangai" structural paragenesis, and the projection of the plume at the level of the lower mantle coincides with the highest part of the Khangai dome (Fig. 13).

It was suggested that the formation of the Khangai and Khentei arches is associated with concentration of the pre-Mesozoic granite masses in their crust [2]. But the areas occupied by granites on these arches do not exceed those around the arches. Even if we assume that the content of granites increases at the deep levels of the Earth's crust, the rise of the arches associated with this would be leveled by the long-term erosion. The Late Cretaceous and Cenozoic basalt volcanism of the arches is of mantle origin. We consider that the rise of the decompacted plume mantle led to the formation of the Khangai and Khentei arches. The upper mantle flows propagating from the plume caused extension and subsidence of the Earth's crust in the belt of basins around the arches.

Extension and softening of the thinned lithosphere above the Khangai plume reduced the effect of plate interactions and, thus, the impact of the Indo-Eurasian collision to the more northern tectonic zones of the region [54]. The geodynamic dominants there are the southern pressure of the Siberian platform and the movement of Transbaikalia and northeastern Mongolia to the SE.

The largest active faults (Tunka-Mondy, Erzin-Agardag, Tsetserleg, Khangai, and Bogd) are superimposed on the structural manifestations of the "Khangai" paragenesis. The low-velocity mantle weakens the lithosphere rheology and makes it more capable of seismic displacement. At the same time, thinning and weakening of the lithosphere reduce the stress that can be accumulated in earthquake source. We propose to solve this contradiction, assuming that the fields of tectonic stress are multicomponent and differ in epochs of relative tectonic quiescence from stress fields that increase from time to time and are realized by significant fault displacement during strong earthquakes [106]. In our case, a long-term stress field could be responsible for the development of the "Khangai" paragenesis, and increasing stress could provide the strongest earthquakes on active fault zones.

The influence of the Khangai plume is expressed over a wider area, where seismic wave velocities in the upper mantle are reduced to a greater or lesser extent. In the Gobi Altai and partly Mongolian Altai, this led to the bending deformation of the basement surface. The decrease in δVp in Western Transbaikalia is partly due to the upper mantle flow propagating from the Khangai plume, but may partly be the result of the impact of events on the eastern active margin of Asia. Previously, data were presented that the Baikal rift zone separates the high-velocity upper mantle of the Siberian Platform from the low-velocity mantle of Transbaikalia, and this low-velocity layer, plunging, continues towards the Sea of Japan [8, 36, 45, 114, 115].

Figures 8, 12, and 13 demonstrate the connection of the Khangai plume with low-velocity volumes of the Transbaikalian mantle and confirm our earlier data [56] that the low-velocity Transbaikalian layer at depths of 450–800 km plunges to the east up to depths of 750–1400 km under the Zeya depression. Through this layer, the low-velocity material could penetrate into Transbaikalia. Thus, the decrease in seismic wave velocities in the mantle of Transbaikalia can be an integral effect of action of the Khangai plume and the Pacific margin.

The localization of manifestations of intraplate volcanism, their composition, structural position, and age are described in numerous publications [6, 38–40, 62, 63, 112, 113]. The intraplate volcanism in the region, which began in the Late Jurassic ca. 160 Ma after the closure of the Transbaikalian part of the Mongolian-Okhotsk Ocean, initially consisted of eruptions of various compositions and was represented by alkaline and subalkaline basalts from the end of the Early Cretaceous to the Holocene.

According to Yarmolyuk et al. [62, 113], the intraplate basaltic volcanism in the region is of different origin, partly associated with rifting. The cited

authors consider the spatial constancy of volcanic manifestations of different ages, which indicates their connection with a stable permanent magmatic source, to be signs of plume volcanism. These authors represent the plumes as hot mantle jets ascending from the hypothetical vast lowest mantle hot volume [10] to the lithosphere, which they destroy with a system of magma channels. The cited authors suggest the presence of such plumes-jets under the volcanic areas of the Gobi Altai – Southern Khangai, Southern Baikal, Western Transbaikalia, and, possibly, the central Aldan Shield.

Our studies do not support the existence of a vast low-velocity volume in the lowest mantle beneath the study region. The Khangai plume rises from depths of no more than 1300 km. The projections of the areas of distribution of the low-velocity mantle volumes onto the land surface cover all fields of the Cretaceous and Cenozoic volcanism. The low-velocity volumes of the sublithospheric mantle, found at a depth of 67 km under the Eastern Tuva, the southern foothills of the Eastern Sayan, and the neighboring part of Mongolia (Fig. 13), correspond to the Late Cenozoic manifestations of volcanism. The Khentei branch of the plume corresponds to an area of the intense Cretaceous volcanism, and the Dariganga Late Cenozoic volcanic field is located above the southeastern part of this low-velocity anomaly. The fields of the Late Cenozoic basaltic volcanism in Transbaikalia are located above the low-velocity mantle volumes, expressed in a horizontal slice 655 km deep (Fig. 13). Thus, the influence of the Khangai plume and its branches on the Cretaceous and Cenozoic intraplate volcanism in the region is proved.

Comparison of the Khangai Plume with Other Mantle Plumes

The Khangai and Tibetan plumes form a single vast volume of the "hot" (low-velocity) mantle and are isolated from each other only in the upper mantle level by a relatively high-velocity dam under the Qaidam and the eastern end of the Tarim microplate. The Tibetan plume is located under the Central and Eastern Tibet to the north of the South Tibetan zone of Lhasa and is close in shape to an overturned cone rising from depths of 1500–1600 km (Figs. 3 and 12). The plume is expressed in the Late Cenozoic structure by a significant uplift of the land surface. No manifestations of plume volcanism were found above it. In the both plumes, δVp slightly increase or the distribution of low-velocity masses becomes discontinuous at the transition layer of the mantle (Figs. 9–12). This is probably due to mineral transformations.

Thus, the Khangai and Tibetan plumes ascend from depths of 1300–1600 km, i.e., from the upper part of the lower mantle. They differ in this from the upper mantle plumes and from the African (Ethiopian-Afar) and Pacific superplumes, although the decrease in seismic velocities is comparable at the upper mantle level in the Khangai and Tibetan plumes and the superplumes and their branches. Analyzing the above relations, we mean the lowering of the MITP08 model resolution in the lower mantle, but, despite it, tracing the "hot" volume deep into the roots of the Khangai and Tibetan plumes is determined quite confidently.

The African and Pacific superplumes ascend from the core-mantle boundary. They have the widest distribution area in the lower mantle, and above they are divided into separate jets. To analyze the global spatial distribution of superplume branches, we chose the NGRAND model [71, 82], which has less, but uniform resolution throughout the entire depth of the mantle. This made it possible to adequately assess the distribution of "hot" and "cold" areas, although with the loss of fine details (Fig. 14).

The African and Pacific superplumes form a pair of antipodal structures located on opposite sides of the spheroid. Their branches rise to the surface with a geometric divergence in the form of overturned cones and upper mantle flows departing from superplumes. The W–E-trending global cross section at latitude 45° N [51] shows two conical zones of tomographic minima of superplumes according to the NGRAND and HWE97 models [71, 82, 108].

The Khangai and Tibetan plumes may have channels of communication with both the Pacific and African superplumes at different mantle depths, but their relationship remains debatable (Figs. 3–7).

The possibility of integral influence of the Khangai plume and the "hot" flow from the Pacific margin on the structure of the mantle in Transbaikalia is expressed in Fig. 10a by two non-contiguous volumes of low-velocity mantle, the isthmus between which at a depth of ca. 1500 km is characterized by the slightly reduced (less than –0.22%) δVp values.

The Tibetan plume may be connected with the branch of the Pacific superplume beneath the Southeast China at the level of the tops of the lower mantle (Fig. 12b). The connection of the Tibetan plume with

Fig. 14. Volumetric model of the African (Ethiopia-Afar) and Pacific superplumes and their branches into Central Asia: (a) – two N–S-trending sections of the block-diagram demonstrate the Pacific (left) and African (right) superplumes; the W–E-trending section shows branches of the Pacific superplume that can be connected with the "hot" mantle of Central Asia; (b) – the right N–S-trending section of the block-diagram demonstrates the Khangai plume and the W–E-trending section shows its possible links with the Pacific superplume branches. Volumetric distribution of the δV_S velocity variations based on the NGRAND tomographic model [71, 82] is shown in several orthogonal vertical sections above the mantle-core boundary (2770 km). The vertical scale is six times more than the horizontal one. The violet contour corresponds to the Khangai plume.

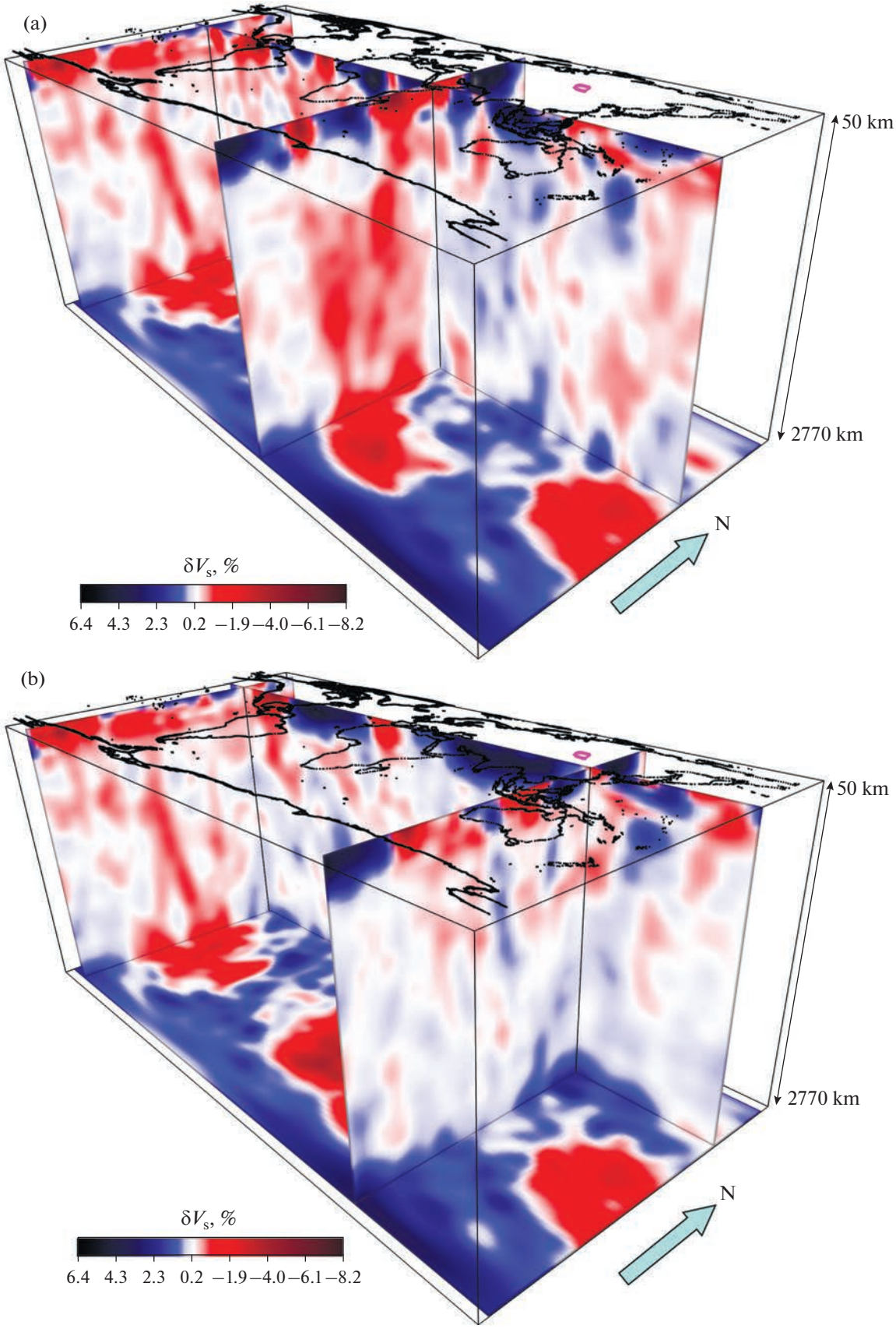
(a)
50 km
2770 km
N
δV_s, %
6.4 4.3 2.3 0.2 −1.9 −4.0 −6.1 −8.2
(b)
50 km
2770 km
N
δV_s, %
6.4 4.3 2.3 0.2 −1.9 −4.0 −6.1 −8.2

the Iranian branch of the African superplume is possible at the level of the upper mantle through the southern part of the Turanian Plate (Figs. 10a and 11b). A possible link between the base of the Tibetan plume and the lower mantle branch of the African plume is seen in Fig. 11a.

The approach of the branches of the African and Pacific superplumes to the region of Central Asia is observed in Fig. 14a. The N–S-trending section passing through the African superplume shows its main and most contrasting elements. The W–E-trending section captures the northern branches of the Pacific superplume, which become less contrasting towards the Central Asia, but their trajectories are traced quite confidently. A cold slab under the Himalayas and Southern Tibet, blocking the upper mantle flow from the African superplume, is also visible (Fig. 11a).

A cross section illustrating The low-velocity branch of the Pacific superplume is seen in the western part of the section shown in Fig. 14a. Figure 13, where the junction of sections is focused in the area of the Khangai plume, demonstrates that the distribution of heated masses of the upper mantle is similar to that shown in Figs. 8–12. A connection with the western branches of the Pacific superplume, which penetrate under Central Asia at depths of ca. 1000 km, is more confidently traced. This configuration is partially visible also in Fig. 8.

The presented relationships of low-velocity mantle volumes show a high probability of the material and energy supply of the Khangai and Tibetan plumes by flows from the African and Pacific superplumes. However, the possibility of independent generation of the Khangai and Tibetan plumes remains. It could be provided by the formation of hydrides of metals and, in particular, of iron with the participation of hydrogen coming from the Earth's core. The iron hydride is stable at temperatures and pressures characteristic of the lower mantle approximately at the level of the base of the Khangai and Tibetan plumes [37].

CONCLUSIONS

The paper demonstrates the results of studies of relationships between the low-velocity mantle volumes of the Khangai plume and the Cenozoic deformation of the Earth's crust in the northern Central Asia. The plume was identified as a result of the analysis of the MITP08 volumetric model of seismic velocity variations δVp. Above the plume, the lithosphere is thinned to ca. 50 km, and especially low velocities ($\delta Vp < -0.6\%$) are found in the sublithospheric mantle up to a depth of 400 km. The main body of the plume covers the Gobi Altai, the Khangai Highland and extends north to Tuva and the southern spurs of the Eastern Sayan. The area of the plume decreases with depth, and its deepest part (1250–1300 km) is located under the southern part of the Khangai Highland. The Khentei branch of the plume was revealed. It is located SE of the Khentei Highlands and connected with the main plume body at depths of 800–1000 km. Flows from the Khangai plume and its Khentei branch extend at different depths to Transbaikalia. At the same time, the volume of the low-velocity mantle in Transbaikalia merges in the east with the branch of the Pacific superplume, i.e., it can be fueled from two sources.

The Khangai uplift of the Earth's crust that has been developing since the Late Mesozoic and reaching a height of 3500–4000 m in the southern part is situated above the center of the main body of the Khangai plume. The contour of the Khangai plume and its Khentei branch is bounded to the SE by a belt of flat Late Cenozoic depressions stretching along the southeastern border of Mongolia. The NE-trending grabens formed in the NE above the low-velocity mantle of Transbaikalia. On the other sides, the Khangai uplift is bounded by the C-shaped belt of intermontane basins separated by low ridges. The belt includes the South Basin of the Baikal rift zone, the Tunka and Tuva basins in the north, the Ubsu-Nur and Big Lakes Basins in the west, and the Valley of Lakes in the south. The basins were filled with lacustrine and alluvial deposits of the Upper Oligocene to Pliocene. In the Quaternary, the South Basin of Baikal became a part of the Baikal rift.

The structural paragenesis of the Khangai arch and surrounding basins is the result of the dynamic impact of the plume. On its territory including the Khentei and Transbaikalia branches, the Cenozoic basaltic plume volcanism is manifested, in some places inheriting Cretaceous volcanic manifestations. This structural paragenesis has developed in the region simultaneously with another structural paragenesis, which is expressed the best of all by the ensemble of active faults and is the result of the lateral interaction of plates and blocks of the lithosphere due to the convergence of the Indian and Siberian platforms and the shifting of Transbaikalian Asia from the Siberian platform.

A deep-seated connection between the Khangai plume and the Tibetan plume, located under the central and eastern parts of the Tibetan plateau to the north of the Lhasa block, was found. The Tibetan plume has the shape of a funnel rising from depths of 1500–1600 km and is accompanied by thinning of the lithospheric mantle and uplift of the land surface. The Khaigai and Tibetan plumes represent a specific category of plume formations whose roots are located in the upper part of the lower mantle. In contrast to them, the African and Pacific superplumes ascend from the boundary between the core and the mantle, are larger, and are accompanied by extended branches at the levels of the upper mantle and the upper part of the lower mantle, which have a global geodynamic impact. The mantle volumes with weak negative δVp have been identified, which can be interpreted as

channels for the entry of material from the both superplumes into the Khangai and Tibetan plumes. We admit also the own sources of formation of these plumes as a result of mineral transformations at the level of their roots.

ACKNOWLEDGMENTS

The authors express their gratitude to the reviewer Academician V.V. Yarmolyuk and the anonymous reviewer for useful comments and to the editor M.N. Shupletsova (Geological Institute of the RAS) for careful editing.

FUNDING

The geological setting of the Cenozoic structures was studies within the theme FMMG-2023-0006 of the Geological Institute of the RAS. The other studies and preparing of the paper were financed by the Russian Science Foundation, Project no. 22-17-00049.

CONFLICT OF INTEREST

The authors of this work declare that they have no conflicts of interest.

REFERENCES

1. S. G. Arzhannikov and A. V. Arzhannikova, "The paleoseismogenic activation of the Great Lakes segment of the Erzin–Agar-Dag fault," Volcanol. Seismol., No. 2, 56–66 (2009).
2. A. V. Arzhannikova, *Doctoral Dissertation in Geology and Mineralogy* (Inst. Zemn. Kory Sib. Otd. Ross. Akad. Nauk, Irkutsk, 2021).
3. A. V. Voznesensky, "The study of the Khangai mining area in 1905 in Northern Mongolia," in *Materials for the Department of Physical Geography,* Vol. 1 (RGO SSSR, Leningrad, 1962).
4. Geology and seismicity of the Baikal-Amur Mainline Zone, in *Neotectonics*, Ed. by N. A. Logachev (Nauka, Novosibirsk, 1984) [in Russian].
5. *Gobi–Altai Earthquake*, Ed. by N. A. Florensov and V. P. Solonenko (Akad. Nauk SSSR, Moscow, 1963) [in Russian].
6. E. V. Devyatkin, The Cenozoic of Inner Asia: Stratigraphy, geochronology, and correlation, in *Transactions of Joint Soviet-Mongolian Geological Expedition* (1981). Vol. 27 (Nauka, Moscow, 1981).
7. E. V. Devyatkin, "Inner Asia," in *Neotectonics, Geodynamics, and Seismicity of Northern Eurasia*, Ed. by A. F. Grachev (Inst. Fiz. Zemli Ross. Akad. Nauk, Moscow, 2000), pp. 92–100.
8. D. Zhao, F. Piraino, and L. Liu, "Mantle structure and dynamics under East Russia and adjacent regions," Russ. Geol. Geophys. **51** (9) 925–938 (2010).
9. S. M. Zamaraev and V. V. Samsonov, "The geological structure and oil-bearing capacities of the Selenga depression," in *Geology and Oil-Bearing Potential of East Siberia* (Gostoptekhizdat, Moscow, 1959), pp. 435–475 [in Russian].
10. L. P. Zonenshain and M.I. Kuzmin, "Intraplate magmatism and its significance for understanding processes in the Earth's mantle," Geotektonika, No. 1, 28–45 (1983).
11. Yu. A. Zorin, T. V. Balk, M. R. Novoselova, and E. Kh. Turutanov, "Thickness of the lithosphere beneath the Baikal rift zone and adjacent regions," Izv. Akad. Nauk SSSR. Ser. Fiz. Zemli, No. 7, 32–42 (1988).
12. Yu. A. Zorin, V. G. Belichenko, E. Kh. Turutanov, A. M. Mazukabzov, E. V. Sklyarov, and V. V. Mordvinova, "Structure of the lithosphere and geodynamics of the western part of the Mongol-Okhotsk Belt," Otech. Geol., No. 11, 52–58 (1997).
13. L. P. Imaeva, V. S. Imaev, B. M. Koz'min, and K. Makkei, "Formation dynamics of fault-block structures in the eastern segment of the Baikal–Stanovoi seismic belt," Izv., Phys. Solid Earth, No. 11, 1–7 (2009).
14. V. M. Kochetkov, S. D. Khil'ko, Yu. A. Zorin, et al., *Seismotectonics and Seismicity of the Cis-Khubsugul Area* (Nauka, Novosibirsk 1993) [in Russian].
15. I. Yu. Kulakov, "Upper mantle structure beneath Southern Siberia and Mongolia from regional seismic tomography," Russ. Geol. Geophys. **49** (3), 187–196 (2008).
16. K. G. Levi, S. M. Babushkin, A. A. Badardinov, V. Yu. Buddo, G. V. Larkin, A. I. Miroshnichenko, V. A. Sankov, V. V. Ruzhich, H. L. Wong, D. Delvaux, and S. Colman, "Active tectonics of the Baikal area," Geol. Geofiz. **36** (10), 154–163 (1995).
17. Lǐ Sìguāng, *Geology of China* (Izd. Inostr. Liter., Moscow, 1952) [in Russian].
18. N. A. Logachev, "History and geodynamics of the Baikal Rift," Russ. Geol. Geophys. **44** (5), 373–387 (2003).
19. N. A. Logachev, I. V. Antoshchenko-Olenev, D. B. Bazarov, V. I. Galkin, G. S. Goldyrev, A. S. Endrikhinskii, A. G. Zolotarev, A. I. Sizikov, and G. F. Ufimtsev, *The Development History of the Topography of Siberia and the Far East. The Highlands of the Baikal Region and Transbaikalia* (Nauka, Moscow, 1974) [in Russian].
20. N. V. Lukina, "Altai–Sayan area of recent ridging of continental lithosphere. Baikal intracontinental rift system," in *Neotectonics and Recent Geodynamics of Mobile Belts*, Ed. by P. N. Kropotkin (Nauka, Moscow, 1988), pp. 276–326 [in Russian].
21. A. V. Luk'yanov, "Structural manifestations of horizontal crustal movements," in *Trans. Geol. Inst. USSR Acad. Sci.,* Vol. 136 (Nauka, Moscow, 1965).
22. O. V. Lunina, *Faults and Seismicity-Induced Geological Processes in the South of the East Siberia and Adjacent Areas* (Sib. Otd Ross. Akad. Nauk, Novosibirsk, 2016) [in Russian].
23. O. V. Lunina and A. S. Gladkov, "Fault pattern and stress field in the Western Tunka rift (southwestern flank of the Baikal rift system)," Russ. Geol. Geophys. **45** (10), 1188–1199 (2004).
24. O. V. Lunina, A. S. Gladkov, and N. N. Nevedrova, *Rift Depressions of the Cis-Baikal: Tectonic Structure and Development History* (GEO, Novosibirsk, 2009) [in Russian].
25. A. V. Lukhnev, V. A. San'kov, A. I. Miroshnichenko, S. V. Ashurkov, and E. Kalais, "GPS rotation and

strain rates in the Baikal–Mongolia region," Russ. Geol. Geophys. **51** (7), 785–793 (2010).
26. V. N. Mazilov, S. A. Kashik, and T. K. Lomonosova, "Oligocene deposits in the Tunka trough (Baikal rift zone)," Geol. Geofiz. **34** (8), 81–88 (1993).
27. V. D. Mats, "The sedimentary fill of the Baikal Basin: Implications for rifting age and geodynamics," Russ. Geol. Geophys. **53** (9), 936–954 (2012).
28. V. D. Mats, G. F. Ufimtsev, M. M. Mandel'baum, A. M. Alekshin, A. V. Pospeev, M. N. Shimaraev, and O. M.Khrustov, *Cenozoic of the Baikal Rift Trough: Structure and Geological History* (GEO, Novosibirsk, 2001) [in Russian].
29. V. I. Mel'nikova and N. A. Radziminovich, "Focal mechanisms of the earthquakes in the Baikal Region for 1991–1996," Geol. Geofiz. **39** (11), 1598–1607 (1998).
30. A. A. Mossakovsky, S. V. Ruzhentsev, S. G. Samygin, and T. N. Kheraskova, "Central Asian Fold Belt: Geodynamic evolution and history of formation," Geotektonika, No. 6, 3–32 (1993).
31. V. G. Nikolaev, L. A. Vanyakin, V. V. Kalinin, and V. E. Milanovsk[illegible]"The structure of the sedimentary cover of Lake Baikal," Byull. MOIP. Otd. Geol. **60** (2), 48–58 (1985).
32. A. N. Ovsyuchenko, Yu. V. Butanaev, and K. S. Kuzhuget, "Paleoseismic seismotectonic study of the node in the south-west of Tuva," Vestn. ONZ RAN **8**, 1–18 (2016).
33. A. N. Ovsyuchenko, Yu. V. Butanaev, A. M. Sugoranova, A. S. Lar'kov, and A. V. Marakhanov, "Research of the Kaakhem system of active faults in Tuva: Segmentation and model of specific earthquakes," Geosfer. Issled., No. 1, 6–16 (2019).
34. A. N. Ovsyuchenko, S. Demberel, Yu. V. Butanaev, N. G. Koshevoi, Ts. Batsaikhan, and N. Baatar, "The Khubsugul earthquake of January 12, 2021, $M_w = 6.7$, Northern Mongolia: Geological effects and tectonic position of the source," Dokl. Earth Sci. **511** (1), 566-570 (2023).
35. L. M. P[illegible]ov, N. A. Bepzin, A. I. Xanchuk, G. Badarch, V. G. Belichenko, A. N. Bulatov, S. I. Dril', G. L. Kirillova, M. I. Kuz'min, W. J. Nocleberg, A. D. Prokopiev, V. F. Timofeev, O. Tomurtogoo, and H. Yan, "Model for the formation of orogenic belts in Central and Northeastern Asia," Tikhookean. Geol. **22** (6), 7–41 (2003).
36. N. N. Puzyrev, M. M. Mandel'baum, S. V. Krylov, et al., "Deep-seated seismic sounding of the Earth's crust and top mantle in the Baikal region," in *Baikal Rift*, Ed. by N. A. Florensov (Nauka, Novosibirsk, 1975), pp. 51–67 [in Russian].
37. Yu. M. Pushcharovskii and D. Yu. Pushcharovskii, *Geology of the Earth's Mantle* (GEOS, Moscow, 2010) [in Russian].
38. S. V. Rasskazov, *The Magmatism of the Baikal Rift System* (Nauka, Novosibirsk, 1993) [in Russian].
39. S. V. Rasskazov, S. B. Brandt, I. S. Brandt, and A. V. Ivanov, *Radioisotope Geology in Tasks and Examples* (GEO, Novosibirsk, 2005) [in Russian].
40. S. V. Rasskazov, H. A. Logachev, I. S. Brandt, S. B. Brandt, and A. B Ivanov, *Geochronology and Geodynamics of the Late Cenozoic: South Siberia and East Asia* (Nauka, Novosibirsk, 2000) [in Russian].
41. S. V. Rasskazov, N. A. Lyamina, G. P. Chernyaeva, I. V. Luzina, A. F. Rudnev, and I. N. Rezanov, *Cenozoic Stratigraphy of the Vitim Plateau: Phenomenon of Long-Term Rifting in the South of East Siberia* (GEO, Novosibirsk, 2007) [in Russian].
42. S. V. Rasskazov, N. A. Lyamina, I. V. Luzina, G. P. Chernyaeva, I. S. Chuvashova, and M. V. Usol'tseva, "Sediments of the Tertiary Tankhoi Field, South Baikal Basin: Stratigraphy, correlation, and structural transformations in the Baikal Region," Geodynam. Tectonophys. **5** (4), 993–1032 (2014).
43. S. V. Rasskazov, V. A. San'kov, V. V. Ruzhich, and O. P. Smekalin, *Cenozoic Continental Rifting: Guide of Geological Excursions in Tunka Rift Basin* (Inst. Zemn. Kory Sib. Otd. Ross. Akad. Nauk, Irkutsk, 2010) [in Russian].
44. E. A. Rogozhin, *Essays on Regional Seismotectonics*, Ed. by A.O. Gliko (Inst. Fiz. Zemli Ross. Akad. Nauk, Moscow, 2012) [in Russian].
45. V. A. Rogozhina, "Zone of reduced velocity of seismic waves in the upper mantle," in *Essays on the Deep Structure of the Baikal Rift*, Ed. by N. A. Florensov (Nauka, Novosibirsk, 1977), pp. 64–78 [in Russian].
46. V. A. San'kov, "Recent geodynamics of intracontinental areas: Instrumental and geomorphological assessment of crustal movements and deformation in Central Asia," Geodynam. Tectonophys. **5** (1), 159–182 (2014).
47. V. A. San'kov and A. A. Dobrynina, "Modern fault formation in the Earth's crust of the Baikal rift system according to the data on the mechanisms of earthquake sources," Dokl. Earth Sci. **465** (1), 1191–1195 (2015).
48. V. A. San'kov, A. V. Lukhnev, A. I. Miroshnichenko, A. A. Dobrynina, S. V. Ashurkov, L. M. Byzov, M. G. Dembelov, E. Calais, and J. Déverchère, "Contemporary horizontal movements and seismicity of the south Baikal Basin (Baikal rift system)," Izv., Phys. Solid Earth **50**, 785–794 (2014).
49. V. A. San'kov, A. V. Parfeevets, A. V. Lukhnev, A. I. Miroshnichenko, and S. V. Ashurkov, "Late Cenozoic geodynamics and mechanical coupling of crustal and upper mantle deformations in the Mongolia–Siberia mobile area," Geotectonics **45** (5), 378–393 (2011).
50. S. Yu. Sokolov, "Tectonics and geodynamics of the equatorial segment of the Atlantic," in *Transactions of Geological Institute of Russian Academy of Sciences*, Vol. 618 (Nauchn. mir, Moscow, 2018).
51. S. Yu. Sokolov, "The depth geodynamic state and its correlation with the surface geological and geophysical parameters along the sublatitudinal profile of Eurasia," Geodynam. Tectonophys. **10** (4), 945–957 (2019).
52. S. Yu. Sokolov, K. O. Dobrolyubova, and N. N. Turko, "Relationships of surface geological and geophysical characteristics with the deep structure of the Mid-Atlantic Ridge according to seismic tomography data," Geotectonics **56** (2), 107–122 (2022).
53. V. G. Trifonov, "Features of the development of active faults," Geotectonics, **2**, 16–26 (1985).
54. V. G. Trifonov, E. A. Zelenin, S. Yu. Sokolov, and D. M. Bachmanov, "Active tectonics of Central Asia," Geotectonics **55**, 361–376 (2021).
55. V. G. Trifonov and V. I. Makarov, "Active faults (Mongolia)," in *Neotectonics and Recent Geodynamics of Mobile Belts* (Nauka, Moscow, 1988), pp. 239–272 [in Russian].

56. V. G. Trifonov, S. Yu. Sokolov, D. M. Bachmanov, S. A. Sokolov, and Ya. I. Trikhunkov, "Neotectonics and deep structure of Central Asia," Geotectonics **55**, 334–360 (2021).
57. G. F. Ufimtsev, *Morphotectonics of the Baikal Rift Zone* (Nauka Novosibirsk, 1992) [in Russian].
58. D. R. Hutchinson, A. Yu. Golmshtok, L. P. Zonenshain, T. C. Moore, C. A. Scholz, and K. D. Klitgord, "Structural features of the sedimentary sequence of Lake Baikal based on the multichannel seismic survey data," Geol. Geofiz. **34** (10–11), 25–36 (1993).
59. S. D. Khil'ko, R. A. Kurushin, V. M. Kochetkov, et al., *Earthquakes and Fundamentals of Seismic Zoning of Mongolia* (Nauka, Moscow, 1985) [in Russian].
60. Yu. G. Tsekhovsky and M. G. Leonov, "Sedimentary formations and main development stages of the western Transbaikal and southeastern Baikal regions in the late Cretaceous and Cenozoic," Lithol. Miner. Resour. **42** (4), 349–362 (2007).
61. L. D. Shorygina, "Stratigraphy of Cenozoic deposits of Western Tuva, in *Transactions of Geological Institute of USSR Academy of Sciences*, Vol. 26 (Akad. Nauk SSSR, Moscow, 1960), pp. 16–202 [in Russian].
62. V. V. Yarmolyuk, V. I. Kovalenko, and V. G. Ivanov, "The intraplate late Mesozoic–Cenozoic volcanic province in central east Asia as a projection of the mantle hot field," Geotektonika, No. 5, 41–67 (1995).
63. V. V. Yarmolyuk, A. V. Nikiforov, A. M. Kozlovskii, and E. A. Kudryashova, "Mesozoic East Asian magmatic province: Structure, magmatic signature, formation conditions," Geotectonics **53**, 500–516 (2019).
64. C. R. Allen, "Geological criteria for evaluating seismicity," Bull. GSA **86** (8), 1041–1057 (1975).
65. M. Amaru, *Global Travel Time Tomography with 3-D Reference Models. Dis. Thesi* (Univ. Utrecht, Germany, 2007, Geol. Ultraiectina. Vol. 274).
66. A. Arzhannikova and S. Arzhannikov, "Morphotectonic and paleoseismological studies of Late Holocene deformation along the Primorsky Fault, Baikal Rift," Geomorphology **342** (1), 140–149 (2019).
67. A. Arzhannikova, S. Arzhannikov, M. Jolivet, R. Vassallo, and A. Chauvet, "Pliocene to Quaternary deformation in South East Sayan (Siberia): Initiation of the Tertiary compressive phase in the southern termination of the Baikal Rift System," J. Asian Earth Sci. **40**, 581–594 (2011).
68. A. Arzhannikova, S. Arzhannikov, J. -F. Ritz, A. Chebotarev, and A. Yakhnenko, "Earthquake geology of the Mondy fault (SW Baikal Rift, Siberia)," J. Asian Earth Sci. **248**, 105614 (2023). https://doi.org/10.1016/j.jseaes.2023.105614
69. A. Arzhannikova, R. Braucher, S. Arzhannikov, G. Aumaitre, D. L. Bourlès, and K. Keddadouche, "The Late Quaternary slip-rate of the Kichera Fault (North Baikal Rift) from morphotectonic, paleoseismological and cosmogenic ^{10}Be analyses," Tectonophysics **812**, 228915 (2021).
70. I. Baljinnyam, A. Bayasgalan, B. A. Borisov, A. Cisternas, M. G. Dem'yanovich, L. Ganbataar, V. M. Kochetkov, R. A. Kurushin, P. Molnar, H. Philip, and Yu. Ya. Vashchilov, *Ruptures of Major Earthquakes and Active Deformation in Mongolia and Its Surrounding* (USA, GSA Mem., 1993, Vol. 181).
71. T. W. Becker and L. Boschi, "A comparison of tomographic and geodynamic mantle models," Geochem. Geophys. Geosyst. **3**, 1–48 (2002).
72. R. K. Bono, J. A. Tarduno, and H. P. Bunge, "Hotspot motion caused the Hawaiian–Emperor Bend and LLSVPs are not fixed," Nature Communications **10**, 3370 (2019).
73. E. Calais, L. Dong, M. Wang, Z. Shen, and M. Vergnolle, "Continental deformation in Asia: a combined GPS solution," Geophys. Rev. Lett. **33**, L24319 (2006).
74. E. Calais, M. Vergnolle, V. San'kov, A. Lukhnev, A. Miroshnitchenko, S. Amarjargal, and J. Déverchère, "GPS measurements of crustal deformation in the Baikal-Mongolia area (1994–2002): Implications for current kinematics of Asia," J. Geophys. Res.: Solid Earth **108** (B10), 1–13 (2003).
75. J.-H. Choi, Ya. Klinger, M. Ferry, J.-F. Ritz, R. Kurtz, M. Rizza, L. Bollinger, B. Davaasambuu, N. Tsend-Ayush, and S. Demberel, "Geologic inheritance and earthquake rupture processes: The 1905 $M \geq 8$ Tsetserleg-Bulnay strike-slip earthquake sequence, Mongolia," J. Geophys. Res.: Solid Earth **123** (2), 1925–1953 (2018).
76. W. D. Cunningham, B. F. Windley, L. A. Owen, T. Barry, D. Dorjnamjaa, and J. Badamgarav, "Geometry and style of partitioned deformation within a late Cenozoic transpressional zone in the eastern Gobi Altai Mountains, Mongolia," Tectonophysics **277** (4), 285–306 (1997).
77. *Database of Active Faults of Eurasia* (GIN RAS, Moscow, 2020). http://neotec.ginras.ru/ database.html (Accessed November 12, 2022).
78. J. De Grave, P. Van den Haute, M. M. Buslov, B. Dehandschutter, and S. Glorie, "Apatite fission-track thermochronology applied to the Chulyshman Plateau, Siberian Altai Region," Radiation Measurements **43**, 38–42 (2008).
79. G. Ding, "Active faults in China", in *A Collection of Papers of International Symposium on Continental Seismicity and Earthquake Prediction (ISCSEP)* (Seismol. Press, Beijing, China, 1984).
80. G. Ding and Y. Lu, "A preliminary discussion on the status of intraplate motions in China," Kexue Tongbao **33** (1), 52–57 (1988).
81. S. S. Gao, P. M. Davis, H. Liu, H. D. Slack, Yu. A. Zorin, V. V. Mordvinova, V. M. Kozhevnikov, and R. P. Meyer, "Seismic anisotropy and mantle flow beneath the Baikal zone," Nature **371**, 149–151 (1994).
82. S. P. Grand, R. D. Van der Hilst, and S. Widiyantoro, "Global seismic tomography: A snapshot of convection in the Earth," GSA Today **7** (4), 1–7 (1997).
83. R. Hall and W. Spakman, "Mantle structure and tectonic history of SE Asia," Tectonophysics **658**, 14–45 (2015).
84. J. Huang and W. P. Chen, "Source mechanisms of the Mogod earthquake sequence of 1967 and the event of 1974 July 4 in Mongolia," Geophys. J. R. Astron. Soc. **84** (2), 361–379 (1986).
85. J. Huang and D. Zhao, "High-resolution mantle tomography of China and surrounding regions," J. Geophys. Res. **111**, B09305 (2006).
86. Zh. Huang and D. Zhao, "Seismotectonics of Mongolia and Baikal Rift zone controlled by lithospheric

structures," Geophys. Rev. Lett. **49** (e2022), 1–10 (2022).
87. M. Jolivet, J.-F. Ritz, R. Vassallo, C. Larroque, R. Braucher, M. Todbileg, A. Chauvet, C. Sue, N. Arnaud, R. De Vicente, A. Arzhanikova, and S. Arzhanikov, "Mongolian summits: An uplifted, flat, old but still preserved erosion surface," Geology **35** (10), 871–874 (2007).
88. Y. Klinger, M. Etchebes, P. Tapponnier, and C. Narteau, "Characteristic slip for five great earthquakes along the Fuyun fault in China," Nat. Geosci. **4**, 389–392 (2011).
89. S. K. Krivonogov and I. Y. Safonova, "Basin structures and sediment accumulation in the Baikal Rift Zone: Implications for Cenozoic intracontinental processes in the Central Asian Orogenic Belt," Gondwana Res. **47**, 267–290 (2017).
90. R. Kurtz, Y. Klinger, M. Ferry, and J. -F. Ritz, "Horizontal surface-slip distribution through several seismic cycles: The Eastern Bogd fault, Gobi-Altai, Mongolia," Tectonophysics **734**, 167–182 (2018).
91. R. A. Kurushin, A. Bayasgalan, M. Ölziybat, B. Enkhtuvshin, P. Molnar, C. Bayarsayhan, K. W. Hudnut, and J. Lin, "The surface rupture of the 1957 Gobi-Altay, Mongolia, earthquake," USA. GSA Spec. Pap. **320** (1997).
92. C. Li, R. D. van der Hilst, E. R. Engdahl, and S. Burdick, "A new global model for P wave speed variations in Earth's mantle," Geochem. Geophys. Geosyst. **9** (5), 1–21 (2008).
93. M. Liu, Y. Yang, Zh. Shen, Sh. Wang, M. Wang, and Y. Wan, "Active tectonics and intracontinental earthquakes in China: The kinematics and geodynamics," USA. GSA Spec. Pap. **425**, 299–318 (2007).
94. P. Molnar and Q. Deng, "Faulting associated with large earthquakes and average rate of deformation in central and eastern Asia," J. Geophys. Res. **89** (B7), 6203–6227 (1984).
95. A. V. Parfeevets and V. A. Sankov, "Late Cenozoic tectonic stress fields of the Mongolian microplate," Geoscience (C. R.) **344**, 227–238 (2012).
96. C. Petit and M. Fournier, "Present-day velocity and stress fields of the Amurian Plate from thin-shell finite-element modelling," Geophys. J. Int. **160** (1), 357–369 (2005).
97. C. Petit, B. Meyer, Y. Gunnell, M. Jolivet, V. San'kov, V. Strak, and N. Gonga-Saholiariliva, "Height of faceted spurs, a proxy for determining long-term throw rates on normal faults: Evidence from the North Baikal Rift System, Siberia," Tectonics **28**, TC6010 (2009).
98. J. -F. Ritz, A. Arzhannikova, R. Vassallo, S. Arzhannikov, C. Larroque, J. -L. Michelot, and M. Massault, "Characterizing the present-day activity of the Tunka and Sayan faults within their relay zone (western Baikal rift system, Russia)," Tectonics **37**, 1376–1392 (2018).
99. J.-F. Ritz, R. Vassallo, R. Braucher, E. T. Brown, S. Carretier, and D. Bourlès, "Using in situ-produced ^{10}Be to quantify active tectonics in the Gurvan Bogd mountain range (Gobi-Altay, Mongolia)," USA. GSA Spec. Pap. **415**, 87–110 (2006).
100. M. Rizza, J. -F. Ritz, R. Braucher, R. Vassallo, C. Prentice, S. Mahan, et al., "Slip rate and slip magnitudes of past earthquakes along the Bogd left-lateral strike-slip fault (Mongolia)," Geophys. J. Int. **186**, 897–927 (2011).
101. M. Rizza, J-F. Ritz, C. Prentice, R. Vassallo, R. Braucher, C. Larroque, A. Arzhannikova, S. Arzhannikov, S. Mahan, M. Massault, J.-L. Michelot, and M. Todbileg, "Earthquake geology of the Bolnay fault (Mongolia)," Bull. Seismol. Soc. Am. **105** (1), 72–93 (2015).
102. A. Schlupp and A. Cisternas, "Source history of the 1905 great Mongolian earthquakes (Tsetserleg, Bolnay)," Geophys. J. Int. **169** (3), 1115–1131 (2007).
103. A. A. Shchetnikov, D. White, I. A. Filinov, and N. Rutter, "Late Quaternary geology of the Tunka rift basin (Lake Baikal region), Russia," J. Asian Earth Sci. **46**, 195–208 (2012).
104. J. Shi, X. Feng, Sh. Ge, Zh. Yang, M. Bo, J. Hu, "The Fuyun earthquake fault zone in Xinjiang, China," in *A Collection of Papers of International Symposium on Continental Seismicity and Earthquake Prediction (ISCSEP)* (Seismol. Press, Beijing, China, 1984), pp. 325–346.
105. P. Tapponnier and P. Molnar, "Active faulting and Cenozoic tectonics of the Tien Shan, Mongolia and Baykal regions," J. Geophys. Res. **84**, 3425–3459 (1979).
106. V. G. Trifonov, A. M. Korzhenkov, and Kh. M. Omar, "Recent geodynamics of major strike-slip zones," Geodes. Geodynam. **6** (5), 361–383 (2015).
107. V. G. Trifonov and M. N. Machette, "The World Map of Major Active Faults Project," Ann. Geofis. **36** (3–4), 225–236 (1993).
108. R. D. Van der Hilst, S. Widiyantoro, and E. R. Engdahl, "Evidence of deep mantle circulation from global tomography," Nature **386** (6625), 578–584 (1997).
109. D. G. Van der Meer, D. J. Van Hinsbergen, and W. Spakman, "Atlas of the underworld: Slab remnants in the mantle, their sinking history, and a new outlook on lower mantle viscosity," Tectonophysics **723**, 309–448 (2018).
110. M. Vergnolle, E. Calais, and L. Dong, "Dynamics of continental deformation in Asia," J. Geophys. Res. **112**, B11403 (2007).
111. Q. Wang, P. -Z. Zhang, J. T. Freymueller, R. Bilham, K. M. Larson, X. Lai, X. You, Zh. Niu, J. Wu, Ya. Li, J. Liu, Zh. Yang, and Q. Chen, "Present-day crustal deformation in China constrained by Global Positioning System measurements," Science **294**, 574–577 (2001).
112. B. F. Windley and M. B. Allen, "Mongolia plateau: Evidence for a late Cenozoic mantle plume beneath central Asia," Geology **21**, 295–298 (1993).
113. V. V. Yarmolyuk, E. A. Kudryashova, A. M. Kozlovsky, V. A. Lebedev, and V. M. Savatenkov, "Late Mesozoic–Cenozoic intraplate magmatism in Central Asia and its relation with mantle diapirism: Evidence from the South Khangai volcanic region, Mongolia," J. Asian Earth Sci. **111**, 604–623 (2015).
114. D. Zhao, J. Lie, T. Inoue, A. Yamada, and S. S. Gao, "Deep structure and origin of the Baikal rift zone," Earth Planet. Sci. Lett. **243**, 681–691 (2006).
115. Yu. A. Zorin, M. R. Novoselova, E. Kh. Turutanov, and V. M. Kozhevnikov, "Structure of the lithosphere of the Mongolian–Siberian mountainous province," J. Geodynam. **11**, 327–342 (1990).

SPELL: OK